NBS

Technical Note 164

ON PLASMA COLLISION FREQUENCIES PROPORTIONAL TO ENERGY IN THE RADIO WAVE REFLECTION AND TRANSMISSION PROCESS

J. R. JOHLER AND JOHN D. HARPER, JR.

U. S. DEPARTMENT OF COMMERCE
NATIONAL BUREAU OF STANDARDS

THE NATIONAL BUREAU OF STANDARDS

Functions and Activities

The functions of the National Bureau of Standards are set forth in the Act of Congress, March 3, 1901, as amended by Congress in Public Law 619, 1950. These include the development and maintenance of the national standards of measurement and the provision of means and methods for making measurements consistent with these standards; the determination of physical constants and properties of materials; the development of methods and instruments for testing materials, devices, and structures; advisory services to government agencies on scientific and technical problems; invention and development of devices to serve special needs of the Government; and the development of standard practices, codes, and specifications. The work includes basic and applied research, development, engineering, instrumentation, testing, evaluation, calibration services, and various consultation and information services. Research projects are also performed for other government agencies when the work relates to and supplements the basic program of the Bureau or when the Bureau's unique competence is required. The scope of activities is suggested by the listing of divisions and sections on the inside of the back cover.

Publications

The results of the Bureau's research are published either in the Bureau's own series of publications or in the journals of professional and scientific societies. The Bureau publishes three periodicals available from the Government Printing Office: The Journal of Research, published in four separate sections, presents complete scientific and technical papers; the Technical News Bulletin presents summary and preliminary reports on work in progress; and the Central Radio Propagation Laboratory Ionospheric Predictions provides data for determining the best frequencies to use for radio communications throughout the world. There are also five series of nonperiodical publications: Monographs, Applied Mathematics Series, Handbooks, Miscellaneous Publications, and Technical Notes.

A complete listing of the Bureau's publications can be found in National Bureau of Standards Circular 460, Publications of the National Bureau of Standards, 1901 to June 1947 ($1.25), and the Supplement to National Bureau of Standards Circular 460, July 1947 to June 1957 ($1.50), and Miscellaneous Publication 240, July 1957 to June 1960 (includes Titles of Papers Published in Outside Journals 1950 to 1959) ($2.25); available from the Superintendent of Documents, Government Printing Office, Washington 25, D.C.

NATIONAL BUREAU OF STANDARDS

Technical Note 164

ISSUED MARCH 1, 1963

ON PLASMA COLLISION FREQUENCIES PROPORTIONAL TO ENERGY IN THE RADIO WAVE REFLECTION AND TRANSMISSION PROCESS

J. R. Johler and John D. Harper, Jr.
Central Radio Propagation Laboratory
National Bureau of Standards
Boulder, Colorado

NBS Technical Notes are designed to supplement the Bureau's regular publications program. They provide a means for making available scientific data that are of transient or limited interest. Technical Notes may be listed or referred to in the open literature.

For sale by the Superintendent of Documents, U.S. Government Printing Office
Washington 25, D.C. Price 40 cents

CONTENTS

FOREWORD

This work was sponsored by the U.S. Air Force as part of Tasks 4 and 5 of the Rome Air Development Center D.O. AF 30 (602)-2488, March 1961.

ABSTRACT

The high conductivity of the ionosphere in large measure determines the propagation of terrestrial radio waves. The ionosphere can be treated theoretically as a magneto-ionic plasma composed of electrons, ions, and neutral particles. Certain macroscopic properties of these particles, such as the complex index of refraction, can be deduced from the microscopic particle statistics of ionized gases. These properties can then be applied directly to Maxwell's equations to determine the reflection and transmission process, provided a suitable composition for the model plasma has been found.

The composition of the real ionosphere is not uniform, especially in the vertical direction. Such nonuniformity can be treated theoretically with the aid of a flexible model ionosphere employing the notion of a continuously stratified plasma.

An extensive survey of both the index of refraction of typical electron-ion plasmas as models of the ionosphere together with the reflection coefficients is made in this paper to determine the significance of the notion of heavy-particle electron-collision frequencies proportional to energy.

The introduction of electron-ion collision frequencies with a linear dependence upon the average value of the Maxwellian particle velocity distribution results in some interesting changes in the detail of the reflection and transmission coefficients at low frequencies. It can be noted, however, that the reflection coefficients determined by application of the continuously stratified notion to particular models of the ionosphere are not drastically changed by the introduction of such electron collisions.

ON PLASMA COLLISION FREQUENCIES PROPORTIONAL TO ENERGY IN THE RADIO WAVE REFLECTION AND TRANSMISSION PROCESS

by

J. Ralph Johler

and

John D. Harper, Jr.

1. INTRODUCTION

Both the reflection and transmission process of a radio wave at an electron-ion plasma have considerable theoretical and practical importance. Thus, theoretical treatment of the reflection process is necessary to describe the field of a radio wave transmitted around the earth by reflections from the ionosphere. Also, the field of a radio wave at a space vehicle either in or above the ionosphere is a timely consideration for the theoretician.

The treatment of a continuously varying medium (varying in one direction, such as the vertical z-direction, Fig. 1) by approximating the medium with one or more slabs of uniform composition has been utilized by many authors, such as Hines [1951], Wait [1953], Ferraro and Gibbons [1959], Brekhovskikh [1960], Johler and Harper [1962], Johler [1962]. This paper applies such techniques to a magneto-ionic

plasma carrying the process to the limit until the increase in the number of slabs and the decrease in the thickness of such slabs result in a convergence to a stable reflection or transmission coefficient.

Recently the work of Phelps [1960] has developed the notion of electron-ion collision frequencies with a linear dependence on the energy exponent of the Maxwellian particle-velocity distribution. This has raised grave questions as to the validity of the use of a constant collision frequency in the classical magneto-ionic theory, especially at low frequencies. This paper introduces the monoenergetic electron collisions (electron collisions proportional to energy) into the analysis of nonuniform plasma reflections and transmissions so that a comparison can be made with the classical magneto-ionic theory, especially at low frequencies. An extensive survey of the index of refraction of an electron-heavy particle magneto-plasma is made together with appropriate reflection coefficients to determine the significance of electron-ion collision frequencies proportional to energy.

2. THE COMPLEX INDEX OF REFRACTION OF THE PLASMA

The complex index of refraction of a non-uniform medium varying in one direction, such as the vertical z-direction, Fig. 2, will be examined in some detail in this paper. This is accomplished by subdividing the medium into slabs of uniform composition. It is

therefore necessary initially to determine the complex index of refraction of each such slab.

The index of refraction of a uniform magneto-ionic plasma can be examined in detail with the aid of the plane coordinate system illustrated, Fig. 1. The xy-plane is situated at the lower boundary of the model plasma defined as a position in space at which the electron density is nil ($N = 0$) and above which ($z > 0$) the ionization varies as some arbitrary function (or profile), $N(z)$, $N(h)$, where h in practice is the height above the terrestrial sphere in radio wave propagation problems. Also, at all $z < 0$, the ionization is assumed to be negligible.

The mathematical description† of the propagation in a magneto-ionic medium can be formulated with the aid of a plane wave, $\overline{E}_i$, incident from the region below the xy-plane ($z < 0$, Fig. 1) at an angle of incidence with the vertical z-direction, ϕ_i,

$$E_i = |\overline{E}_i| \exp [i (\omega t - \frac{\omega}{c} \eta D)] \qquad (1)$$

where the field is assumed to be a time-harmonic wave oscillating in time, t, at a frequency, $f = \omega / 2\pi$, with c the speed of light, $c \sim 3(10^8)$ meter/second, and η the index of refraction, which for a vacuum, $\eta = \eta_o = 1$, and $D = \eta_o D = x \sin \phi_i \sin \phi_a + y \sin \phi_i \cos \phi_a + z \cos \phi_i$. (2)

The magnetic azimuth, ϕ_a, is reckoned clockwise from magnetic north, Fig. 1, i.e., from the yz-plane, which contains the static

† Rationalized MKS units are used throughout this paper.

magnetic field vector, $\overline{\mathcal{H}}$, oriented at a dip or inclination angle relative to the horizontal, I. A resultant wave, $\overline{E}_t$, transmitted into the model ionosphere magneto-ionic plasma ($z > 0$) is then assumed to have the form,

$$E_t = |\overline{E}_t| \exp[i(\omega t - \frac{\omega}{c} \eta D)], \tag{3}$$

where in the plasma,

$$\eta D = x \sin \phi_i \sin \phi_a + y \sin \phi_i \cos \phi_a + z \zeta, \tag{4}$$

in which ζ is in general a complex number, the value of which will depend upon the altitude, z, and on $\zeta = \zeta(z)$, since the complex index of refraction, η,

$$\eta^2 = \zeta^2 + \sin^2 \phi_i, \tag{5}$$

varies with the electron-ion composition which in turn changes with altitude.

The complex index of refraction, η, can be determined locally at a particular altitude by a simultaneous solution of Maxwell's equations,

$$\overline{\nabla} \times \overline{E} + \mu_o \frac{\partial \overline{H}}{\partial t} = 0,$$

$$\overline{\nabla} \times \overline{H} - \overline{J} - \epsilon_o \frac{\partial \overline{E}}{\partial t} = 0, \tag{6}$$

where $\overline{E}$ and $\overline{H}$ are the electric (volts/meter) and magnetic (ampere-turns/meter) fields, $\overline{J} = -Ne\overline{V}$ the vector convection current (amperes/square meter),

and the Langevin equation of motion of an electron,

$$m\frac{d\bar{V}}{dt} + mg\,\bar{V} + \mu_o e\,(\bar{V} \times \bar{\mathcal{H}}) + e\bar{E} = 0, \tag{7}$$

in which m is the electronic mass, e the electronic charge, μ_o the permeability of space ($\mu_o = 4\pi(10^{-7})$ henry/meter), $\bar{\mathcal{H}}$ the vector static magnetic field (ampere-turns/meter), $\bar{V}$ is the vector velocity, and g is the collision frequency parameter (seconds $^{-1}$). The elimination of the vectors $\bar{J}$ and $\bar{H}$ from the simultaneous solution of equations (6, 7) results in the matrix equation, using the Cartesian coordinates of Fig. 1,

$$\begin{bmatrix} a_{11} & a_{12} & a_{13} \\ a_{21} & a_{22} & a_{23} \\ a_{31} & a_{32} & a_{33} \end{bmatrix} \begin{bmatrix} E_x \\ E_y \\ E_z \end{bmatrix} = 0, \tag{8}$$

where the coefficients will be defined in Appendix I.

If the field E, equation (8), exists the determinant of the matrix must vanish. Expansion of the determinant yields a quartic equation in ζ [Booker, 1939], [Johler and Harper, 1962],

$$a_4\zeta^4 + a_3\zeta^3 + a_2\zeta^2 + a_1\zeta + a_o = 0, \tag{9}$$

with coefficients also defined in Appendix I.

The Booker [1939] quartic equation (9) is quite significant, since the four complex roots of such an equation describe four indexes of refraction, $\eta = \eta_{o,e}^{i,r}$ corresponding to upgoing (i) with negative imaginary part (Im $\eta < 0$) and downgoing (r) with positive imaginary part (Im $\eta > 0$) together with ordinary (o) and extraordinary (e) for each upgoing or downgoing magneto-ionic propagation component. The intensity and phase of these propagation components are dependent upon direction of propagation relative to the direction of the static-magnetic field, $\bar{H}$, (Fig. 1) which acts on the convection currents, $\bar{J}$, as the Lorentz force, equation (7),

$$-\frac{\mu_o}{N}(\bar{J} \times \bar{H}) = \mu_o e (\bar{V} \times \bar{H}).$$

Such a medium of propagation is said to be anisotropic. Indeed, the ionosphere which surrounds the earth is one such plasma medium.

3. BOUNDARY CONDITIONS

The detailed structure of the flexible plasma model is illustrated, Fig. 2, as a stack of plasma slabs of arbitrary thickness (except for the topmost slab of thickness $z_p = \infty$). The number of such slabs, p, and the thickness is quite flexible, since the idea of this analysis is that the measured electron density-altitude and collision frequency-altitude (N(z) and $\nu(z)$, respectively) profiles can be

approximated to any desired accuracy by decreasing z_n and increasing p simultaneously until a stable reflection process is obtained.

A constant electron density, collision frequency, and static magnetic field with respect to altitude, z, is of course assumed for each slab, z_n, and associated with each such slab a set of four roots, $\zeta = \zeta_n$, is found to exist. Two of the roots will exhibit a negative imaginary part (Im ζ negative), corresponding to an upgoing propagation component (+ z direction, Figs. 1 and 2). Also, two of these roots will exhibit a positive imaginary part (Im ζ positive), corresponding to a downgoing propagation component (-z direction, Figs. 1 and 2). Except for the topmost slab, it is necessary to consider both upgoing and downgoing components in this analysis.

The treatment of a continuously varying medium, i.e., one which varies in the vertical z-direction, Figs. 1 and 2, with one or more slabs of uniform composition was presented in a previous paper [Johler and Harper, 1962] . Indeed, the technique was carried to the limit at which the number of slabs, p, for each calculation depends upon the computation precision required and the particular values of the electric and geometric parameters. Reflection and transmission coefficients were calculated, and the stratification process was continued for model electron density and collision frequency profiles until a stable reflection or transmission was obtained. It was therefore

demonstrated, that subject to the provision that a convergence could be demonstrated numerically, the stratified model could be employed to represent a continuum, hence the notion of continuous stratification.

The distinction between an ordinary and an extraordinary propagation component is ambiguous and obscure in the nonuniform ionosphere. Indeed, if only the reflection coefficient is of interest the distinction is immaterial. However, if the progress of the wave upward through the ionosphere is to be examined in detail, the distinction should be maintained to avoid a confusing analysis. This is accomplished by an examination of the form of the index of refraction function with respect to frequency and altitude (or electron density and collision frequency which vary with respect to altitude). Thus, the complex index of refraction, equation (5), is detailed for each frequency and slab, z_n, $\eta = \eta_n$, and the upgoing (i) ordinary and extraordinary $\eta^{(n)}_{i,\ o,\ e}$ and the downgoing (r) ordinary and extraordinary $\eta^{(n)}_{r,\ o,\ e}$ function continuity is examined in detail as a function of frequency to determine the crossover point of the function for each slab or electron density under consideration. The Re η was employed in this analysis. Thus, above the crossover point the ordinary wave was considered to be the greater of the two roots, Re η_o > Re η_e, and below the crossover point the ordinary wave was

considered to be the lesser of the two roots, $\mathrm{Re}\ \eta_o < \mathrm{Re}\ \eta_e$. At precisely the crossover point, the two, of course, are identical, $\eta_o = \eta_e$. This point, for examples with low electron density examined in this analysis, was found to be below the plasma frequency, $f_N = \omega_N/2\pi$. The absolute distinction between the two propagation components remains quite arbitrary, but the analysis must be consistent between each slab and consistent within each slab for upgoing and downgoing propagation components to simplify the detailed study of the wave progress in the ionosphere. The almost random possibility as to order in which the four components emerge in the numerical solution [Johler and Walters, 1960] of the quartic equation (9) (the Muller [1956] iterative procedure was employed) makes necessary this logical procedure for sorting out the roots thus obtained.

The boundaries of each slab are introduced as an expression for the continuity of the tangential $\bar{E}$ and $\bar{H}$ fields and the normal $\bar{\bar{H}}$ fields at each boundary, Fig. 2, of the model plasma. This is accomplished by equating the field immediately above and immediately below each boundary which, after considerable ado, can be expressed in concise form as the matrix equation (10),

$$
\begin{bmatrix}
a_{1,1} & a_{1,2} & a_{1,3} & a_{1,4} & a_{1,5} & a_{1,6} & & & & & & & & & & \\
b_{1,1} & b_{1,2} & b_{1,3} & b_{1,4} & b_{1,5} & b_{1,6} & & & & & & & & & & \\
c_{1,1} & c_{1,2} & c_{1,3} & c_{1,4} & c_{1,5} & c_{1,6} & & & & & & & & & & \\
d_{1,1} & d_{1,2} & d_{1,3} & d_{1,4} & d_{1,5} & d_{1,6} & & & & & & & & & & \\
 & a_{2,3} & a_{2,4} & a_{2,5} & a_{2,6} & a_{2,7} & a_{2,8} & a_{2,9} & a_{2,10} & & & & & & & \\
 & b_{2,3} & b_{2,4} & b_{2,5} & b_{2,6} & b_{2,7} & b_{2,8} & b_{2,9} & b_{2,10} & & & & & & & \\
 & c_{2,3} & c_{2,4} & c_{2,5} & c_{2,6} & c_{2,7} & c_{2,8} & c_{2,9} & c_{2,10} & & & & & & & \\
 & d_{2,3} & d_{2,4} & d_{2,5} & d_{2,6} & d_{2,7} & d_{2,8} & d_{2,9} & d_{2,10} & & & & & & & \\
 & & & & & a_{3,7} & a_{3,8} & a_{3,9} & a_{3,10} & a_{3,11} & a_{3,12} & a_{3,13} & a_{3,14} & & & \\
 & & & & & b_{3,7} & b_{3,8} & b_{3,9} & b_{3,10} & b_{3,11} & b_{3,12} & b_{3,13} & b_{3,14} & & & \\
 & & & & & c_{3,7} & c_{3,8} & c_{3,9} & c_{3,10} & c_{3,11} & c_{3,12} & c_{3,13} & c_{3,14} & & & \\
 & & & & & d_{3,7} & d_{3,8} & d_{3,9} & d_{3,10} & d_{3,11} & d_{3,12} & d_{3,13} & d_{3,14} & & & \\
 & & & & & & & & & \cdots & \cdots & \cdots & \cdots & & & \\
 & & & & & & & & & \cdots & \cdots & \cdots & \cdots & & & \\
 & & & & & & & & & \cdots & \cdots & \cdots & \cdots & & & \\
 & & & & & & & & & \cdots & \cdots & \cdots & \cdots & & & \\
 & & & & & & & & & & & & & a_{p,p+4} & \cdots & a_{p,p+9} \\
 & & & & & & & & & & & & & b_{p,p+4} & \cdots & b_{p,p+9} \\
 & & & & & & & & & & & & & c_{p,p+4} & \cdots & c_{p,p+9} \\
 & & & & & & & & & & & & & d_{p,p+4} & \cdots & d_{p,p+9}
\end{bmatrix}
\begin{bmatrix}
T_{em}, T_{mm} \\
T_{ee}, T_{me} \\
U^{(1)}_{eio}, U^{(1)}_{mio} \\
U^{(1)}_{eie}, U^{(1)}_{mie} \\
U^{(1)}_{ero}, U^{(1)}_{mro} \\
U^{(1)}_{ere}, U^{(1)}_{mre} \\
U^{(2)}_{eio}, U^{(2)}_{mio} \\
U^{(2)}_{eie}, U^{(2)}_{mie} \\
U^{(2)}_{ero}, U^{(2)}_{mro} \\
U^{(2)}_{ere}, U^{(2)}_{mre} \\
\cdot \quad \cdot \\
\cdot \quad \cdot \\
\cdot \quad \cdot \\
\cdot \quad \cdot \\
U^{(p-1)}_{eio}, U^{(p-1)}_{mio} \\
U^{(p-1)}_{eie}, U^{(p-1)}_{mie} \\
U^{(p-1)}_{ero}, U^{(p-1)}_{mro} \\
U^{(p-1)}_{ere}, U^{(p-1)}_{mre} \\
U^{(p)}_{eio}, U^{(p)}_{mio} \\
U^{(p)}_{eie}, U^{(p)}_{mie}
\end{bmatrix}
+
\begin{bmatrix}
a_{oe}, a_{om} \\
b_{oe}, b_{om} \\
c_{oe}, c_{om} \\
d_{oe}, d_{om}
\end{bmatrix}
= 0
\tag{10}
$$

where the elements a_{11} ... can be deduced as a consequence of these boundary conditions with results as shown in Appendix II, provided the reflection coefficients, T, and the transmission coefficients, U, T', are defined,

$$
T_{ee} = \frac{E_{y'r}}{E_{y'i}} \qquad T'_{ee} = \frac{E_{y't}}{E_{y'i}} \qquad U^{(n)}_{eio} = \frac{E^{(n)}_{yio}}{E_{y'i}} \qquad U^{(n)}_{ero} = \frac{E^{(n)}_{yro}}{E_{y'i}}
$$

$$
T_{em} = \frac{E_{x'r}}{E_{y'i}} \qquad T'_{em} = \frac{E_{x't}}{E_{y'i}} \qquad U^{(n)}_{mio} = \frac{E^{(n)}_{yio}}{E_{x'i}} \qquad U^{(n)}_{mro} = \frac{E^{(n)}_{yro}}{E_{x'i}}
$$

$$
T_{me} = \frac{E_{y'r}}{E_{x'i}} \qquad T'_{me} = \frac{E_{y't}}{E_{x'i}} \qquad U^{(n)}_{eie} = \frac{E^{(n)}_{yie}}{E_{y'i}} \qquad U^{(n)}_{ere} = \frac{E^{(n)}_{yre}}{E_{y'i}}
$$

$$
T_{mm} = \frac{E_{x'r}}{E_{x'i}} \qquad T'_{mm} = \frac{E_{x't}}{E_{x'i}} \qquad U^{(n)}_{mie} = \frac{E^{(n)}_{yie}}{E_{x'i}} \qquad U^{(n)}_{mre} = \frac{E^{(n)}_{yre}}{E_{x'i}}
\tag{11}
$$

where, Fig. 2, n = 1, 2, 3..., p-1, p, and the four T' are defined as a transmission coefficient into a topmost slab of infinite extent, z, and zero electron density, $N = 0$, $\eta_p = \eta_o = 1$.

The reflection coefficients, T_{ee}, T_{em}, T_{me}, T_{mm}, describe the reflection into the region below the model plasma, $z < 0$. Thus, T_{ee} refers to vertical electric polarization of the incident wave and a corresponding vertical electric polarization of the reflected wave. T_{em} refers to the generation of the abnormal component (horizontal electric polarization) by the incident vertical electric wave. Similarly, T_{mm} refers to vertical magnetic incident wave and vertical magnetic reflected wave, and T_{me} refers to a corresponding abnormal component (horizontal magnetic).

The transmission coefficients, U, refer to transmission at the particular point in the ionosphere under investigation to which the wave has penetrated. There are four propagation components and two polarizations and, hence, eight types of transmission coefficients: upgoing and downgoing, ordinary and extraordinary, vertical electric and vertical magnetic.

Thus, the nature of the wave reflected from the plasma, the nature of the wave transmitted through the plasma, and indeed the nature of the wave progressing within the plasma are completely described by the coefficients determined by this analysis.

4. CLASSICAL MAGNETO-IONIC THEORY

The Booker [1939] quartic equation (9) is satisfied by the famous Appleton-Hartree formula [Appleton, 1932], [Hartree, 1929, 1931],

$$\eta^2 = 1 - \frac{\frac{2}{s}\left(1 - \frac{1}{s}\right)}{2\left(1-\frac{1}{s}\right) - \frac{h^2}{s^2}\sin^2\psi \pm \sqrt{\frac{h^2}{s^2}\sin^4\psi + 4\frac{h^2}{s^2}\left(1 - \frac{1}{s}\right)^2\cos^2\psi}}, \tag{12}$$

where, $\zeta^2 = \eta^2 - \sin^2\phi_i$, (13)

provided,

$$\cos\psi = -\frac{\zeta}{\eta}\sin I + \frac{1}{\eta}\sin\phi_i\cos\phi_a\cos I, \tag{14}$$

or,

$$\sin\psi = \frac{1}{\eta}\left[\eta^2 - \zeta^2\sin^2 I - \sin\phi_i\cos\phi_a\left(\sin\phi_i\cos\phi_a\cos^2 I - 2\zeta\sin I\cos I\right)\right]^{\frac{1}{2}} \tag{15}$$

This formula, employing real ψ, has become identified with the classical magneto-ionic theory. This solution becomes identical with the Booker quartic with complex ψ [Johler and Walters, 1960], i.e., the propagation direction relative to the earth's magnetic field is in general complex, $\psi = \mathrm{Re}\,\psi + i\,\mathrm{Im}\,\psi$.

5. ELECTRON COLLISION FREQUENCIES PROPORTIONAL TO ENERGY

The particle statistics of the electron-ion gas with superposed electrodynamic and magnetostatic fields has been investigated in some detail since the classical magneto-ionic theory was introduced (1932). Most of these studies have arrived at macroscopic properties from the well known Maxwell-Boltzmann theory by means of approximations of the Boltzmann equation. The Langevin equation (7) for constant collision, $g \sim \nu$, is one such approximation. The re-examination of the classical magneto-ionic theory in recent years can be traced to the work of Huxley [1937, 1938, 1940], Pfister [1955], Jancel and Kahan [1955], Dingle, Arndt and Roy [1956], Molmud [1959], Allis [1956], and Sen and Wyller [1960]. Particular emphasis, based on experimental work with gases in the laboratory, has been placed by Phelps [1960] on the dependence of the collision process upon the energy, $au^{j/2}$, where $u = kT/e$ (k = Boltzmann's constant, T = temperature, degrees kelvin, and e = electronic charge), with special emphasis on the linear dependence, $j = 2$, on the collision frequency, $\nu = \nu(u) = au$, where a is a constant. This linear dependence of the collision frequency, $\nu(u)$, upon energy has been called a monoenergetic electron collision process. Phelps [1960] anticipated grave consequences as to the general validity of the classical magneto-ionic theory. This paper, therefore, has introduced collision

frequencies proportional to energy into the analysis of the reflection coefficient, and the consequences of such a theory are examined.

Phelps [1960] has developed integrals of the electron velocity or conductivity tensor. The integration over a Maxwellian energy distribution expressed in terms of energy, $eu = \frac{1}{2} m V^2$, or, $f_o = [e/\pi k T]^{\frac{3}{2}} \exp[-eu/k T]$, involves momentum transfer collisions with gas molecules proportional to the energy u, $\nu = \nu(u)$ and can be accomplished for a continuous electromagnetic wave of angular frequency, $\omega = 2\pi f$.

The notion of a complex parameter, g, in the Langevin equation (7) was introduced by Molmud [1959]. Thus, in the classical theory, $g \sim \nu$. In the monoenergetic theory the parameter $g = f(\nu(u))$ is a complex and frequency-dependent number. The implication of the classical magneto-ionic theory that such a quantity can be represented by a real effective value without a frequency dependence is therefore not in general valid concept.

The derivation of the parameter, g, and its introduction into the analysis is given in Appendix III.

6. COMPUTATIONS AND DISCUSSION

The precise model for the lower ionosphere has been the subject of extensive investigation. Such a model can be presented as an electron density-altitude, N(h) or N(z), Fig. 2, profile together with a collision frequency-altitude profile. Two such models, N(h) or N(z) profiles, are illustrated, Fig. 3. The Houston Composite [Waynick, 1957] represents the approximate condition of the ionosphere at daytime-noon. A profile which was measured with a rocket sounding by Sedden and Jackson [1958] is also illustrated, Fig. 3. This model is representative of the condition of the lower ionosphere during a local auroral-zone blackout of the type confined to the auroral zone or some segment thereof. Measurements were not made to establish this model below 1000 electron/cm^3. However, various methods have been proposed to extrapolate such models to lower electron densities. The Chapman theory of ionized-layer formation can be written, Chapman [1931, 1939] , Budden [1961] ,

$$N = N_o \exp \tfrac{1}{2} \left[1 - \frac{z - z_o}{S} - \sec \chi \exp \left\{ - \frac{z - z_o}{S} \right\} \right], \qquad (50)$$

where $N_o = N_{max} / (\cos \chi)^{\frac{1}{2}}$

$z_o = z_{max} - S \ln (\sec \chi)$

$S = RT/Mg$

R is the gas constant, M is the mean molecular weight, T is the absolute temperature, g is the acceleration of gravity, and χ is the zenith angle of the sun. The scale height, S, can in practice be adjusted to fit measured profiles provided N_{max} and z_{max} are determined by such profiles. The gaussian extrapolation formula is often employed, [Budden, 1955], for the daytime-noon profiles, in which $N_o = N_{max}$, $z_o = z_{max}$,

$$N = N_{max} \exp [- (z - z_{max})^2/k'],$$

where the constant k' is adjusted for best fit of the measured profile. This latter procedure was followed in the ionosonde blackout model profile illustrated, Fig. 3. Obviously, a variety of other measured or theoretical profiles could be selected. These profiles were employed primarily to demonstrate the techniques described in this paper. The analysis of a variety of other profiles is reserved for future work.

Numerous $\nu(z)$ profiles, both theoretical and measured, based upon the classical magneto-ionic theory, are also available in the literature. Some of these illustrated, Fig. 4, have been deduced by Nicolet [1958], Fejer [1955], Crompton, Huxley, and Sutton [1953], Gardner and Pawsey [1953], and Sedden and Jackson [1958]. The results of Sedden and Jackson [1958] indicate the

theoretical values of Nicolet should be divided by 3, hence the Nicolet/3 $\nu(z)$ profile. The Nicolet/3 $\nu(z)$ profile was selected for the analysis presented in this paper. The collision frequency can be deduced from experimental measurements at high frequencies, (HF). Thus, for example, Kane [1960] employed a frequency 7.75 Mc/s together with the sixth harmonic as a reference and measured the relative attenuation of the ordinary and extraordinary waves, from transmitters in a rocket traveling upward through the D-region. These attenuations are dependent on Im $\eta_{o,e}$, or

$$\exp\left[-\frac{\omega}{c}\ \mathrm{Im}\ \eta_{o,e} D\right].$$

The theoretical calculations of Im $\eta_{o,e}$ at 7.75 Mc/s and 2.0 Mc/s employing the roots $\zeta_{o,e}$ of the quartic equation (9) in equation (5) to determine $\eta_{o,e}$ and using an arbitrary value, N = 500, is illustrated, Figs. 5 and 6, for classical and monoenergetic theory. This implies that the numbers ν for the abscissa of the graphs are constant average values of ν for the classical curve and proportional to energy, u, or $\nu = \nu(u)$ for the monoenergetic curve. Upon selecting a value on the monoenergetic curves for ordinary and extraordinary, and keeping Im η constant and moving over to the classical curve, one notes a change $\frac{\nu}{\nu(u)} \sim 2.5$ for collision frequency values 10^4 to 10^7 approximately, which is in agreement with the deductions of

Kane [1960]. The values of the Nicolet/3 curve, Fig. 4, based on the classical theory were therefore reduced by a factor of 2.5 when used in the monoenergetic theory, $\nu = \nu(u)$. It is interesting to note that the Nicolet/3 curve then agrees quite well with one of the curves of Kane [1960] deduced with the aid of monoenergetic theory from rocket measurements.

Reflection coefficients, T_{ee}, T_{em}, T_{me}, T_{mm}, which can be employed to determine the field strength of a radio wave at the surface of the earth [Johler, 1961c] were evaluated with the aid of the models, Figs. 3, 4, and the continuously stratified technique, Fig. 2.

The results of the calculation of the reflection coefficients based on the monoenergetic theory are compared with the results based on the classical theory as a function of frequency for grazing incidence on the ionosphere, $\phi_i \sim 82^\circ$, ($d \sim 1000$ statute miles for a single ionosphere reflection [Johler, 1961c], using the Houston composite model, Fig. 3. A magnetic inclination or dip, $I = 60^\circ$, was employed, and the results for propagation into the east, magnetic azimuth, $\phi_a = 90^\circ$, Fig. 7, and propagation into the west, $\phi_a = 270^\circ$ Fig. 8, are illustrated. In view of the grave consequences anticipated by the introduction of the electron collisions proportional to

energy it is most remarkable that the curves of the classical theory differ only in detail from those of the monoenergetic theory. Indeed, for the models employed in this analysis no new gross phenomenon in the propagation were described by the monoenergetic theory. However, some of the detailed changes are of considerable interest. Thus, for example, at 100 kc/s there is a noteworthy difference between the abnormal components, $T_{em} \sim T_{me}$, based on classical theory as compared with monoenergetic theory. This suggests comparison of loop and vertical antenna measurements at grazing incidence for first ionospheric reflected wave from a vertical radiator type transmitter, for example, to check the monoenergetic theory experimentally.

Similarily, the reflection coefficients, T, based on monoenergetic and classical theories were compared with the blackout model profile N(z), Fig. 3, employing the same (Nicolet/3) model $\nu(h)$ profile, Fig. 4, as shown in Figs. 9 and 10 for propagation into the east ($\phi_a = 90^o$) and propagation into the west ($\phi_a = 270^o$). The geometric-optical angle of incidence, ϕ_i, was, of course, adjusted slightly to take account of the lowering of the ionosphere. Here again, the difference between monoenergetic and classical are only those of small detail. The greatest effect seems again to be in the abnormal components, $T_{em} = T_{me}$.

The reflection coefficient as a function of angle of incidence, ϕ_i, which is related to geometric-optical ray distance subtended along surface of the earth between transmitter and receiver [Johler, 1961c] d, statute miles as shown by the additional abscissa, is illustrated for the quiescent model using the monoenergetic theory, Figs. 11, 12. The results for propagation into the east, $\phi_a = 90°$, Fig. 11, can be compared with the results for propagation into the west, $\phi_a = 270°$, Fig. 12. The particular case of a reflection coefficient for vertical polarization of transmitter and receiver, T_{ee} (vertical electric incident wave and corresponding vertical electric reflected wave), is illustrated as a function of distance, d, or angle of incidence, ϕ_i, in Fig. 13 as a comparison, employing the Houston Composite model, Fig. 3, of east-west, $\phi_a = 270°$ with west-east, $\phi_a = 90°$ propagation together with a comparison of monoenergetic with classical magneto-ionic theories. Thus, at grazing incidence, $\phi_i \sim 82°$, $d \sim 10^3$ miles, $|T_{ee}|$ monoenergetic and classical results exhibit a greater field intensity for propagation into the east as compared with propagation into the west. This is consistent with previous conclusions based on classical theory, only [Johler and Harper, 1962], [Johler, 1961a], [Johler and Walters, 1960], [Johler, 1961c]. For both monoenergetic theory and classical theory both curves cross in the vicinity of Brewster's angle ($d \sim 250$), where at short distances or near vertical

incidence the propagation into the west is more favorable than the propagation into the east for this particular orientation of the earth's magnetic field, I = 60°, ϕ_a = 90°, 270°. The fields predicted by the classical theory are less than those predicted by the monoenergetic theory for propagation into the west. However, for propagation into the east there is a cross-over in the curves as a function of angle of incidence, ϕ_i, or distance, d. A distinguishing feature of these curves when compared with ordinary sharp-boundary-type Fresnel reflection coefficients is the multiple Brewster angles instead of a single Brewster angle (between d = 90 and 300). This can be interpreted physically as multiple regions within the ionosphere of large contribution to the total reflection coefficient. Thus, each such region would exhibit a slightly different Brewster angle since the electron-ion composition of the ionosphere varies with altitude, z.

Figures 14-25 illustrate the complex indexes of refraction representative of low, medium, and high electron densities. The collision-frequency parameter also affects the shape of the curves. Those chosen were associated with the Houston Composite N(h) profile in the reflection coefficient analyses. Grazing incidence, $\phi_i \sim 82°$ is assumed, and the earth's magnetic field, $\mathcal{H}$ = 0.5 gauss, is oriented such that ϕ_a = 0°, and I = 60°.

In making a comparison of the indexes derived from the monoenergetic theory with those derived from the classical theory, perhaps the most noteworthy observation is the lack of major differences. In fact, as the electron density is increased the two cannot be separated graphically. This would, in large measure, account for the only minor changes in the reflection coefficients exhibited by the monoenergetic theory.

An interesting feature of both the monoenergetic and classical index curves is the tendency, as the electron density is increased, for one or both of the extraordinary propagation components to evanesce as a function of frequency (i.e., the point of evanescence, Re $\eta = 0$) although not at the same place.

7. CONCLUSIONS

The continuously stratified concept together with measured or theoretical N(h), ν(h) profiles of the ionosphere can be employed to analyze a variety of conditions of the ionosphere at LF. The introduction of electron collision frequencies proportional to energy into the magneto-ionic theory introduces some interesting changes in the detail of the reflection coefficients and index of refraction of the lower ionosphere. However, the classical theory demonstrates the principal features of the reflection process with remarkable accuracy in view of the grave consequences anticipated by the introduction of electron collisions proportional to energy.

The introduction of electron collision frequencies proportional to energy provides a more accurate description of the macroscopic properties of a magneto-ionic plasma. The comparative simplicity with which such collision frequencies can be introduced into the full-wave solution for the ionosphere warrants their use in describing the detailed reflection or transmission process.

Boulder, Colorado, March 29, 1962.
(Revised August 8, 1962).

8. REFERENCES

Allis, W. P. (1956) Motions of ions and electrons, Handbuch der Physik, edited by S. Flugge (Springer-Berlin), 21, Electron emission, 383-444.

Appleton, E. V. (1932) Wireless studies of the ionosphere, J. Inst. Elec. Engrs. (London), 71, 642.

Barron, D. W. (March 1961) The numerical solution of differential equations governing the reflection of long radio waves from the ionosphere, IV, Proc. Roy. Soc., 260, Ser. A., No. 302.

Booker, H. G. (November 1934) Some general properties of the formulae of the magneto-ionic theory, Proc. Roy. Soc. (London), A 147, 352-382.

Booker, H. G. (1939) Propagation of wave packets incident obliquely upon a stratified doubly refracting ionosphere, Phil. Trans. Roy. Soc., London, Ser. A, 237, 411-451.

Bremmer, H. (1949) Terrestrial radio waves -- theory of propagation, Elsevier Publ. Co., Inc., N.Y., N.Y.

Brekhovskikh, L. M. (1960) Waves in layered media, Academic Press, Inc., New York, N.Y.

Budden, K. G. (1955) The numerical solution of the differential equations governing the reflection of long radio waves from the ionosphere, II, Phil. Trans. Roy. Soc., London, A 248, 45-72.

Budden, K. G. (February 1955) The numerical solution of differential equations governing reflexion of long radio waves from the ionosphere, Proc. Roy. Soc., Ser. A, 227, No. 1171, 516-537.

Budden, K. G. (1961) Radio Waves in the Ionosphere, Cambridge at the University Press, Cambridge, England.

Chapman, S. (1931) The absorption and dissociative or ionizing effect of monochromatic radiation in an atmosphere on a rotating earth, Proc. Phys. Soc. 42, 20-45.

Chapman, S. (1931) The production of ionization by monochromatic radiation incident upon a rotating atmosphere, Part I, Proc. Phys. Soc. 43, 26.

Chapman, S. (1931) The production of ionization by monochromatic radiation incident upon a rotating atmosphere, Part II, Grazing Incidence, Proc. Phys. Soc., 43, 483.

Chapman, S. (1939) The atmospheric height distribution of band absorbed solar radiation, Proc. Phys. Soc., 51, 93.

Crompton, R. W., L. C. H. Huxley, and D. J. Sutton (July 1953) Experimental studies of the motions of slow electrons in air with applications to the ionosphere, Proc. Roy. So . (London) A 218, 507-519.

Dingle, R. B., D. Arndt, and S. K. Roy (1956) The integrals $\xi_p(x)$ and $D_p(x)$ and their tabulation, Appl. Sci. Research, 6 B, 155-164.

Fejer, J. A. (Dec. 1955) The interaction of pulsed radio waves in the ionosphere, J. Atmospheric and Terrest. Phys., 7, 322-332.

Ferraro, A. J. and J. J. Gibbons (1959) Polarization computations by means of multislab approximation, J. Atmospheric and Terrest. Phy., 16, 131.

Gardner, F. F. and J. L. Pawsey (July 1953) Study of the ionospheric D-region using partial reflections, J. Atmospheric and Terrest. Physics, 3, 321-344.

Hartree, D. R. (1929) The propagation of electromagnetic waves in a stratified medium, Proc. Cambridge Phil. Soc. 25, 97.

Hartree, D. R. (1931) The propagation of electromagnetic waves in a refracting medium in a magnetic field, Proc. Cambridge Phil. Soc. 27, 143.

Hines, C. O. (Mar., June - Dec. 1951) Wave packets, the Poynting vector and evergy flow, Pts. I-IV, J. Geophys. Research, 56.

Huxley, L. G. H. (1937) Motions of electrons in gases in electric and magnetic fields, Phil. Mag., 7-Ser., 23, 210-230.

Huxley, L. G. H. (1937) Motions of electrons in magnetic fields and alternating electric fields, Phil. Mag., 7-Ser., 23, 442-464.

Huxley, L. G. H. (1940) The propagation of electromagnetic waves in an ionized atmosphere, Phil. Mag., 7-Ser., 29, 313-329.

Jancel, R. and T. Kahan (February 1955) Theorie du couplage des ondes electromagnetiques ordinaire et extraordinaire dans un plasma inhomogene et anisotrope et conditions de reflexion applications a L'ionosphere, Le Journal de Physique et Le Radium, 16, 136-145.

Johler, J. R. (Jan. - Feb. 1961a) Magneto-ionic propagation phenomena in low- and very-low-radiofrequency waves reflected by the ionosphere, J. Research, NBS, 65D, (Radio Prop.) No. 1, 53-65.

Johler, J. R. (1961b) On LF ionospheric phenomena in radio navigation systems, Avionics Panel Meeting of the Advisory Group for Aeronautical Research and Development (AGARD), 3-8 October 1960, Istanbul, Turkey, or Oranisation du Traite de Atlantique Nord, Pergamon Press, 64, rue de Varenne, Paris 7eme.

Johler, J. R. (Sept. - Oct. 1961c) On the analysis of LF ionospheric phenomena, J. Research NBS, 65D, (Radio Prop.), No. 5, 507.

Johler, J. R. and J. D. Harper, Jr. (Jan. - Feb. 1962) Reflection and transmission of radio waves at a continuously stratified plasma with arbitrary magnetic induction, J. Research NBS, 66D, (Radio Prop.) No. 1, 81-99.

Johler, J. R. and L. C. Walters (May-June 1960) On the theory of reflection of low- and very-low-radiofrequency waves from the ionoshpere, J. Research, NBS, No. 3, 269-285.

Johler, J. R. (2-6 July 1962) On radio wave reflections at a continuously stratified plasma with collisions proportional to energy and arbitrary magnetic induction; International Conference on the Ionosphere, London, England, Physical Society - Institute of Physics.

Kane, J. A. (Feb. 1959) Arctic measurements of electron collision frequencies in the D-region of the ionosphere, J. Geophys. Research, 64, No. 2, 133-139.

Kane, J. A. (Nov. 1960) Re-evaluation of ionospheric electron densities and collision frequencies derived from rocket measurements of refractive index and attenuation, IGY Rocket Report No. 6, 135, National Acad. Sci., Washington, D.C.

Molmud, P. (Apr. 1959) Langevin equation and the ac conductivity of non-Maxwellian plasmas, J. Phys. Res., 114, No. 1, 29-32.

Muller, D. E. (1956) A method for solving algebraic equations using an automatic computer, Math Tables and Other Aids to Computation, 10, No. 53-56, 208.

Nicolet, M. (Apr. 1958) Aeronomic conditions in the mesosphere and lower ionosphere, Science Report No. 102, Pennsylvania State Univ., Univ. Park, Pennsylvania.

Pfister, W. (1955) Studies of the refractive index in the ionosphere: the effect of the collision frequency and of ions, Phys. Soc. of London, Physics of the Ionosphere, Cavendish Lab., Cambridge, England, 394-401.

Phelps, A. V. (Oct. 1960) Propagation constants for electromagnetic waves in weakly ionized, dry air, J. of Applied Physics, 21, No. 10, 1723-1729.

Ratcliffe, J. A. (1959) The Magneto-Ionic Theory and Its Applications to the Ionosphere, A Monograph, Cambridge at the University Press, Cambridge, England.

Seddon, J. C. and J. E. Jackson (July 1958) Rocket Arctic ionosphere measurements, IGY Rocket Report Series, No. 1, 140 148.

Wait, J. R. (1953) Fields of a line current source over a stratified conductor, Applied Science Research, 33.

Wait, J. R. (Mar. - Apr. 1960) Terrestrial propagation of VLF radio waves, J. Research NBS, 64D (Radio Prop.), No. 2.

Wait, J. R. (Apr. - June 1961) Some boundary value problems involving plasma media, J. Research NBS, 65B, (Math and Math Phys.), No. 2, 137-150.

Waynick, A. H. (June 1957) The present state of knowledge concerning the lower ionosphere, Proc. IRE, 45, No. 6, 741-749.

APPENDIX I

The elimination of the vectors, $\bar{J}$ and $\bar{H}$, from the simultaneous solution of Maxwell's equations and the Langevin equation of motion of the electron gives

$$\begin{bmatrix} a_{11} & a_{12} & a_{13} \\ a_{21} & a_{22} & a_{23} \\ a_{31} & a_{32} & a_{33} \end{bmatrix} \begin{bmatrix} E_x \\ E_y \\ E_z \end{bmatrix} = 0,$$

where,

$$a_{11} = 1 - a_L^2 - \zeta^2 - \frac{s}{s^2-h^2}, \quad a_{21} = a_L a_T + i\,\frac{h_L}{s^2-h^2},$$

$$a_{12} = a_L a_T - i\,\frac{h_L}{s^2-h^2}, \qquad a_{22} = 1 - \zeta^2 - a_T^2 - \frac{s^2-h_T^2}{s(s^2-h^2)},$$

$$a_{13} = a_T\zeta + i\,\frac{h_T}{s^2-h^2}, \qquad a_{23} = a_L\zeta + \frac{h_L h_T}{s(s^2-h^2)},$$

$$a_{31} = a_T\zeta - i\,\frac{h_T}{s^2-h^2},$$

$$a_{32} = a_L\zeta + \frac{h_L h_T}{s(s^2-h^2)},$$

$$a_{33} = 1 - a^2 - \frac{s^2-h_L^2}{s(s^2-h^2)}.$$

If the field, $\bar{E}$, exists the determinant of the matrix must vanish, which determinant upon expansion yields a quartic equation in ζ [Booker, 1939], [Johler and Harper, 1962],

$$a_4\zeta^4 + a_3\zeta^3 + a_2\zeta^2 + a_1\zeta + a_o = 0,$$

where,

$$a_0 = (a^2-1)^2\left[1 - \frac{s}{s^2-h^2}\right] + (a^2-1)\left[\frac{1}{s} + \frac{s-2}{s^2-h^2} + \frac{a_L^2 h_T^2}{s(s^2-h^2)}\right] + \frac{s-1}{s(s^2-h^2)},$$

$$a_1 = 2\frac{h_L h_T a_L}{s(s^2-h^2)}(a^2-1),$$

$$a_2 = \left\{2\left[1 - \frac{s}{s^2-h^2}\right] + \frac{h_L^2}{s(s^2-h^2)}\right\}(a^2-1) + \frac{h_T^2 a_L^2}{s(s^2-h^2)} + \frac{s-2}{s^2-h^2} + \frac{1}{s},$$

$$a_3 = 2\frac{h_L h_T a_L}{s(s^2-h^2)} = -a_1 \sec^2 \phi_i,$$

$$a_4 = 1 - \frac{s^2-h_L^2}{s(s^2-h^2)},$$

$$s = \frac{\omega^2}{\omega_N^2}\left[1 - i\frac{\nu}{\omega}\right],$$

$$h = \frac{\omega_H}{\omega_N}\frac{\omega}{2},$$

$h_L = - h \sin I,$

$h_T = h \cos I,$

$a_L = \sin \phi_i \cos \phi_a, \quad a_T = \sin \phi_i \sin \phi_a$

$a = \sin \phi_i$

$\omega_N^2 = Ne^2/\epsilon_o m$

the plasma frequency,

$\omega_H = \mu_o e \mathcal{H}/m, \qquad \mathcal{H} = |\overline{\mathcal{H}}|,$

the gyro frequency,

$\epsilon_o = 1/c^2 \mu_o,$

and where $N = N_n$ the median value of electron density in the interval z_n corresponding to the uniform slab number n, Fig. 2 provided the approximation $g \sim \nu$ or $g_n \sim \nu_n$ for each slab of ordered number n, can be made, i.e., the classical magneto-ionic theory is assumed by a real constant value of collision frequency, ν. Model electron density profiles, N(z), and collision frequency profiles, $\nu(z)$, are shown in Figs. 3 and 4. Such profiles are considered to be representative of daytime noon and local auroral zone blackout conditions of the earth's ionosphere, and therefore have considerable practical significance to radio wave propagation science.

APPENDIX II

The coefficients of the matrix equation (10) can be written:

$$a_{1,1} = \cos \phi_a \qquad b_{1,1} = - \sin \phi_a$$

$$a_{1,2} = - \cos \phi_1 \sin \phi_a \qquad b_{1,2} = - \cos \phi_i \cos \phi_a$$

$$a_{1,3} = - Q^{(1)}_{io} \qquad b_{1,3} = - 1$$

$$a_{1,4} = - Q^{(1)}_{ie} \qquad b_{1,4} = - 1$$

$$a_{1,5} = - Q^{(1)}_{ro} \qquad b_{1,5} = - 1$$

$$a_{1,6} = - Q^{(1)}_{re} \qquad b_{1,6} = - 1$$

$$a_{2,3} = - a_{1,3} \exp\left[-i \frac{\omega}{c} z_1 \zeta^{(1)}_{io}\right] \qquad b_{2,3} = \exp\left[-i \frac{\omega}{c} z_1 \zeta^{(1)}_{io}\right]$$

$$a_{2,4} = - a_{1,4} \exp\left[-i \frac{\omega}{c} z_1 \zeta^{(1)}_{ie}\right] \qquad b_{2,4} = \exp\left[-i \frac{\omega}{c} z_1 \zeta^{(1)}_{ie}\right]$$

$$a_{2,5} = - a_{1,5} \exp\left[-i \frac{\omega}{c} z_1 \zeta^{(1)}_{ro}\right] \qquad b_{2,5} = \exp\left[-i \frac{\omega}{c} z_1 \zeta^{(1)}_{ro}\right]$$

$$a_{2,6} = - a_{1,6} \exp\left[-i \frac{\omega}{c} z_1 \zeta^{(1)}_{re}\right] \qquad b_{2,6} = \exp\left[-i \frac{\omega}{c} z_1 \zeta^{(1)}_{re}\right]$$

$$a_{2,7} = - Q^{(2)}_{io} \qquad b_{2,7} = - 1$$

$$a_{2,8} = - Q^{(2)}_{ie} \qquad b_{2,8} = - 1$$

$$a_{2,9} = - Q^{(2)}_{ro} \qquad b_{2,9} = - 1$$

$$a_{2,10} = - Q^{(2)}_{re} \qquad b_{2,10} = - 1$$

$$a_{3,7} = - a_{2,7} \exp\left[-i \frac{\omega}{c} z_2 \zeta_{io}^{(2)}\right] \qquad b_{3,7} = \exp\left[-i \frac{\omega}{c} z_2 \zeta_{io}^{(2)}\right]$$

$$a_{3,8} = - a_{2,8} \exp\left[-i \frac{\omega}{c} z_2 \zeta_{ie}^{(2)}\right] \qquad b_{3,8} = \exp\left[-i \frac{\omega}{c} z_2 \zeta_{ie}^{(2)}\right]$$

$$a_{3,9} = - a_{2,9} \exp\left[-i \frac{\omega}{c} z_2 \zeta_{ro}^{(2)}\right] \qquad b_{3,9} = \exp\left[-i \frac{\omega}{c} z_2 \zeta_{ro}^{(2)}\right]$$

$$a_{3,10} = - a_{2,10} \exp\left[-i \frac{\omega}{c} z_2 \zeta_{re}^{(2)}\right] \qquad b_{3,10} = \exp\left[-i \frac{\omega}{c} z_2 \zeta_{re}^{(2)}\right]$$

$$a_{3,11} = - Q_{io}^{(3)} \qquad b_{3,11} = - 1$$

$$a_{3,12} = - Q_{ie}^{(3)} \qquad b_{3,12} = - 1$$

$$a_{3,13} = - Q_{ro}^{(3)} \qquad b_{3,13} = - 1$$

$$a_{3,14} = - Q_{re}^{(3)} \qquad b_{3,14} = - 1$$

....

$$a_{p,p+4} = -a_{p-1,p+4} \exp\left[-i \frac{\omega}{c} z_{p-1} \zeta_{io}^{(p-1)}\right] \qquad b_{p,p+4} = \left[-i \frac{\omega}{c} z_{p-1} \zeta_{io}^{(p-1)}\right]$$

....

$$a_{p,p+9} = - Q_{ie}^{(p)} \qquad b_{p,p+9} = - 1$$

$$c_{1,1} = - \cos \phi_i \sin \phi_a \qquad d_{1,1} = - \cos \phi_i \cos \phi_a$$

$$c_{1,2} = - \cos \phi_a \qquad d_{1,2} = \sin \phi_a$$

$$c_{1,3} = - [a_L P_{io}^{(1)} - \zeta_{io}^{(1)} \qquad d_{1,3} = - [\zeta_{io}^{(1)} Q_{io}^{(1)} - a_T P_{io}^{(1)}]$$

$$c_{1,4} = -\left[a_L P_{ie}^{(1)} - \zeta_{ie}^{(1)}\right] \qquad d_{1,4} = -\left[\zeta_{ie}^{(1)} Q_{ie}^{(1)} - a_T P_{ie}^{(1)}\right]$$

$$c_{1,5} = -\left[a_L P_{ro}^{(1)} - \zeta_{ro}^{(1)}\right] \qquad d_{1,5} = -\left[\zeta_{ro}^{(1)} Q_{ro}^{(1)} - a_T P_{ro}^{(1)}\right]$$

$$c_{1,6} = -\left[a_L P_{re}^{(1)} - \zeta_{re}^{(1)}\right] \qquad d_{1,6} = -\left[\zeta_{re}^{(1)} Q_{re}^{(1)} - a_T P_{re}^{(1)}\right]$$

$$c_{2,3} = -c_{1,3} \exp\left[-i\frac{\omega}{c} z_1 \zeta_{io}^{(1)}\right] \qquad d_{2,3} = -d_{1,3} \exp\left[-i\frac{\omega}{c} z_1 \zeta_{io}^{(1)}\right]$$

$$c_{2,4} = -c_{1,4} \exp\left[-i\frac{\omega}{c} z_1 \zeta_{ie}^{(1)}\right] \qquad d_{2,4} = -d_{1,4} \exp\left[-i\frac{\omega}{c} z_1 \zeta_{ie}^{(1)}\right]$$

$$c_{2,5} = -c_{1,5} \exp\left[-i\frac{\omega}{c} z_1 \zeta_{ro}^{(1)}\right] \qquad d_{2,5} = -d_{1,5} \exp\left[-i\frac{\omega}{c} z_1 \zeta_{ro}^{(1)}\right]$$

$$c_{2,6} = -c_{1,6} \exp\left[-i\frac{\omega}{c} z_1 \zeta_{re}^{(1)}\right] \qquad d_{2,6} = -d_{1,6} \exp\left[-i\frac{\omega}{c} z_1 \zeta_{re}^{(1)}\right]$$

$$c_{2,7} = -\left[a_L P_{io}^{(2)} - \zeta_{io}^{(2)}\right] \qquad d_{2,7} = -\left[\zeta_{io}^{(2)} Q_{io}^{(2)} - a_T P_{io}^{(2)}\right]$$

$$c_{2,8} = -\left[a_L P_{ie}^{(2)} - \zeta_{ie}^{(2)}\right] \qquad d_{2,8} = -\left[\zeta_{ie}^{(2)} Q_{ie}^{(2)} - a_T P_{ie}^{(2)}\right]$$

$$c_{2,9} = -\left[a_L P_{ro}^{(2)} - \zeta_{ro}^{(2)}\right] \qquad d_{2,9} = -\left[\zeta_{ro}^{(2)} Q_{ro}^{(2)} - a_T P_{ro}^{(2)}\right]$$

$$c_{2,10} = -\left[a_L P_{re}^{(2)} - \zeta_{re}^{(2)}\right] \qquad d_{2,10} = -\left[\zeta_{re}^{(2)} Q_{re}^{(2)} - a_T P_{re}^{(2)}\right]$$

$$c_{3,7} = -c_{2,7} \exp\left[-i\frac{\omega}{c} z_2 \zeta_{io}^{(2)}\right] \qquad d_{3,7} = -d_{2,7} \exp\left[-i\frac{\omega}{c} z_2 \zeta_{io}^{(2)}\right]$$

$$c_{3,8} = -c_{2,8} \exp\left[-i\frac{\omega}{c} z_2 \zeta_{ie}^{(2)}\right] \qquad d_{3,8} = -d_{2,8} \exp\left[-i\frac{\omega}{c} z_2 \zeta_{ie}^{(2)}\right]$$

$$c_{3,9} = - c_{2,9} \exp\left[-i \frac{\omega}{c} z_2 \zeta_{ro}^{(2)}\right] \qquad d_{3,9} = - d_{2,9} \exp\left[-i \frac{\omega}{c} z_2 \zeta_{ro}^{(2)}\right]$$

$$c_{3,10} = - c_{2,10} \exp\left[-i \frac{\omega}{c} z_2 \zeta_{re}^{(2)}\right] \qquad d_{3,10} = - d_{2,10} \exp\left[-i \frac{\omega}{c} z_2 \zeta_{re}^{(2)}\right]$$

$$c_{3,11} = - [a_L P_{io}^{(3)} - \zeta_{io}^{(3)}] \qquad d_{3,11} = - [\zeta_{io}^{(3)} Q_{io}^{(3)} - a_T P_{io}^{(3)}]$$

$$c_{3,12} = - [a_L P_{ie}^{(3)} - \zeta_{ie}^{(3)}] \qquad d_{3,12} = - [\zeta_{ie}^{(3)} Q_{ie}^{(3)} - a_T P_{ie}^{(3)}]$$

$$c_{3,13} = - [a_L P_{ro}^{(3)} - \zeta_{ro}^{(3)}] \qquad d_{3,13} = - [\zeta_{ro}^{(3)} Q_{ro}^{(3)} - a_T P_{ro}^{(3)}]$$

$$c_{3,14} = - [a_L P_{re}^{(3)} - \zeta_{re}^{(3)}] \qquad d_{3,14} = - [\zeta_{re}^{(3)} Q_{re}^{(3)} - a_T P_{re}^{(3)}]$$

....

$$c_{p,p+4} = -c_{p-1,p+4} \exp\left[-i \frac{\omega}{c} z_{p-1} \zeta_{io}^{(p-1)}\right] \qquad d_{p,p+4} = -d_{p-1,p+4} \exp\left[-i \frac{\omega}{c} z_{p-1} \zeta_{io}^{(p-1)}\right]$$

....

$$c_{p,p+9} = -[a_L P_{ie}^{(p)} - \zeta_{ie}^{(p)}] \qquad d_{p,p+9} = - [\zeta_{ie}^{(p)} Q_{ie}^{(p)} - a_T P_{ie}^{(p)}]$$

$$a_{oe} = \cos \phi_i \sin \phi_a \qquad a_{om} = \cos \phi_a$$

$$b_{oe} = \cos \phi_i \cos \phi_a \qquad b_{om} = - \sin \phi_a$$

$$c_{oe} = - \cos \phi_a \qquad c_{om} = \cos \phi_i \sin \phi_a$$

$$d_{oe} = \sin \phi_a \qquad d_{om} = \cos \phi_i \cos \phi_a .$$

Field ratios in the plasma are of considerable interest.

Defining,

$$P = \frac{E_z}{E_y} ,$$

$$Q = \frac{E_x}{E_y} ,$$

equation (8) can be written,

$$\begin{bmatrix} b_{11} & b_{12} \\ b_{21} & b_{22} \end{bmatrix} \begin{bmatrix} Q \\ P \end{bmatrix} + \begin{bmatrix} b_{10} \\ b_{20} \end{bmatrix} = 0$$

where, $b_{11} = a_{11} \quad a_{11} \quad a_{21}$

$b_{12} = a_{13} \quad a_{13} \quad a_{33}$

$b_{21} = a_{21}$ or a_{31} or a_{31}

$b_{22} = a_{23} \quad a_{33} \quad a_{33}$

$b_{10} = a_{12} \quad a_{12} \quad a_{22}$

$b_{20} = a_{22} \quad a_{32} \quad a_{32}$ respectively,

or, for example,

$$Q = \frac{-\left[1-a^2-\frac{s^2-h_L^2}{s(s^2-h^2)}\right]\left[a_L a_T - i\frac{h_L}{s^2-h^2}\right] + \left[a_T\zeta + i\frac{h_T}{s^2-h^2}\right]\left[a_L\zeta + \frac{h_L h_T}{s(s^2-h^2)}\right]}{\left[1-a^2-\frac{s^2-h_L^2}{s(s^2-h^2)}\right]\left[1-a_L^2-\zeta^2-\frac{s}{s^2-h^2}\right] - \left[a_T\zeta + i\frac{h_T}{s^2-h^2}\right]\left[a_T\zeta - i\frac{h_T}{s^2-h^2}\right]}$$

$$P = \frac{-\left[a_L\zeta + \frac{h_T h_L}{s(s^2-h^2)}\right]\left[1-a_L^2-\zeta^2-\frac{s}{s^2-h^2}\right] + \left[a_L a_T - i\frac{h_L}{s^2-h^2}\right]\left[a_T\zeta - i\frac{h_T}{s^2-h^2}\right]}{\left[1-a^2-\frac{s^2-h_L^2}{s(s^2-h^2)}\right]\left[1-a_L^2-\zeta^2-\frac{s}{s^2-h^2}\right] - \left[a_T\zeta + i\frac{h_T}{s^2-h^2}\right]\left[a_T\zeta - i\frac{h_T}{s^2-h^2}\right]}$$

where the particular slab (Fig. 1), $n = 1, 2, 3, \ldots p-1, p$, under consideration is designated by the notation, $\zeta = \zeta^{(n)}$, $P = P^{(n)}$, $Q = Q^{(n)}$. Since there are four roots to the quartic, the field ratios equations (27, 28) are $P_{io}^{(n)}, P_{ie}^{(n)}, P_{ro}^{(n)}, P_{re}^{(n)}, Q_{io}^{(n)}, Q_{ie}^{(n)}, Q_{ro}^{(n)}, Q_{re}^{(n)}$, corresponding to the zetas (ζ) for upgoing and downgoing (i, r), ordinary and extraordinary (o, e) propagation components in the particular region, z_n, of the electron-ion magnetic plasma under consideration.

APPENDIX III

The velocity, $\bar{V}$, tensor can be written,

$$J = -NeV = \begin{bmatrix} A_1 & A_2 & A_3 \\ B_1 & B_2 & B_3 \\ C_1 & C_2 & C_3 \end{bmatrix} \begin{bmatrix} E_x \\ E_y \\ E_z \end{bmatrix}, \qquad (1)$$

where

$$A_1 = \frac{s(i\omega\epsilon_0)}{s^2-h^2}, \quad B_1 = \frac{-ih_L(i\omega\epsilon_0)}{s^2-h^2}, \quad C_1 = \frac{ih_T(i\omega\epsilon_0)}{s^2-h^2},$$

$$A_2 = \frac{ih_L(i\omega\epsilon_0)}{s^2-h^2}, \quad B_2 = \frac{-(h_T^2 - s^2)(i\omega\epsilon_0)}{s(s^2-h^2)}, \quad C_2 = \frac{-h_L h_T(i\omega\epsilon_0)}{s(s^2-h^2)},$$

$$A_3 = \frac{-ih_T(i\omega\epsilon_0)}{s^2-h^2}, \quad B_3 = \frac{-h_L h_T(i\omega\epsilon_0)}{s(s^2-h^2)}, \quad C_3 = \frac{(s^2-h_L^2)(i\omega\epsilon_0)}{s(s^2-h^2)}. \qquad (2)$$

The coefficients of the tensor matrix can be reduced to the form

$$A_1 = \left[\frac{(-\frac{1}{2})}{g(\Omega_1) + i\Omega_1} + \frac{(-\frac{1}{2})}{g(\Omega_2) + i\Omega_2} \right] (-\omega_N^2 \epsilon_0),$$

$$A_2 = \left[\frac{(\frac{-i}{2} \sin I)}{g(\Omega_1) + i\Omega_1} + \frac{(\frac{i}{2} \sin I)}{g(\Omega_2) + i\Omega_2} \right] (-\omega_N^2 \epsilon_0),$$

$$A_3 = \left[\frac{(\frac{-i}{2} \cos I)}{g(\Omega_1) + i\Omega_1} + \frac{(\frac{i}{2} \cos I)}{g(\Omega_2) + i\Omega_2} \right] (-\omega_N^2 \epsilon_0),$$

$$B_1 = \left[\frac{(\frac{i}{2} \sin I)}{g(\Omega_1) + i\Omega_1} + \frac{(\frac{-i}{2} \sin I)}{g(\Omega_2) + i\Omega_2} \right] (-\omega_N^2 \epsilon_0),$$

$$B_2 = \left[\frac{(-\cos^2 I)}{g(\Omega_0) + i\Omega_0} + \frac{(-\frac{1}{2} \sin^2 I)}{g(\Omega_1) + i\Omega_1} + \frac{(-\frac{1}{2} \sin^2 I)}{g(\Omega_2) + i\Omega_2} \right] (-\omega_N^2 \epsilon_0),$$

$$B_3 = \left[\frac{(\sin I \cos I)}{g(\Omega_0) + i\Omega_0)} + \frac{(-\frac{1}{2} \sin I \cos I)}{g(\Omega_1) + i\Omega_1} + \frac{(-\frac{1}{2} \sin I \cos I)}{g(\Omega_2) + i\Omega_2} \right] (-\omega_N^2 \epsilon_0),$$

$$C_1 = \left[\frac{(\frac{i}{2} \cos I)}{g(\Omega_1) + i\Omega_1} + \frac{(-\frac{i}{2} \cos I)}{g(\Omega_2) + i\Omega_2} \right] (-\omega_N^2 \epsilon_0),$$

$$C_2 = \left[\frac{(\sin I \cos I)}{g(\Omega_0) + i\Omega_0} + \frac{(-\frac{1}{2} \sin I \cos I)}{g(\Omega_1) + i\Omega_1} + \frac{(-\frac{1}{2} \sin I \cos I)}{g(\Omega_2) + i\Omega_2} \right] (-\omega_N^2 \epsilon_0),$$

$$C_3 = \left[\frac{(-\sin^2 I)}{g(\Omega_0) + i\Omega_0} + \frac{(-\frac{1}{2} \cos^2 I)}{g(\Omega_1) + i\Omega_1} + \frac{(-\frac{1}{2} \cos^2 I)}{g(\Omega_2) + i\Omega_2} \right] (-\omega_N^2 \epsilon_0), \qquad (3)$$

where $B_1 = -A_2$, $C_1 = -A_3$, $C_2 = B_3$, and where $\Omega_0 = \omega$, $\Omega_1 = \omega + \omega_H$, $\Omega_2 = \omega - \omega_H$.

The complex, frequency-dependent parameter, g, in the equation of motion (7) is found by integrating over the velocity distribution for electron collision frequencies, $\nu(u) = (\text{constant})(u)$, at each frequency, $\Omega = \Omega_o, \Omega_1, \Omega_2$:

$$g = \left[-\frac{4\pi}{3} \int_o^\infty \frac{u^{3/2}}{[\nu(u) + i\,\Omega]} \frac{\partial}{\partial u} \left\{ \left(\frac{e}{\pi k T} \right)^{3/2} \exp(-eu/kT)\, du \right\} \right]^{-1} - i\,\Omega, \quad (4)$$

which can be written in terms of Dingle, Arndt, and Roz [1956] tabulated functions, $\xi_{5/2}(\chi)$, $\xi_{3/2}(\chi)$:

$$g = \left\{ \frac{1}{\Omega} \left[\frac{5}{2} \left(\frac{1}{\Upsilon} \right) \xi_{5/2} \left(\frac{1}{\Upsilon} \right) - i \left(\frac{1}{\Upsilon 2} \right) \xi_{3/2} \left(\frac{1}{\Upsilon} \right) \right] \right\}^{-1} - i\,\Omega \quad (5)$$

where $\Upsilon = \nu(u)/\Omega$, $u = kT/e$, and $\nu(u) = akT/e = au$. Thus, the implication of the classical magneto-ionic theory, $g \sim \nu$, a constant, real number, is not in general a valid notion, if an energy dependence

$\nu = \nu(u)$ is admitted.

The complex collision frequency, g, can be introduced into the analysis by evaluating the coefficients of the quartic (Appendix I) follows:

$$a_4 = -\omega^2\epsilon_0^2 (C_3 + i\omega\epsilon_0), \tag{6}$$

$$a_3 = -2\omega^2 \epsilon_0^2 a_L B_3, \tag{7}$$

$$a_2 = \omega^2 \epsilon_0^2 [A_1 + B_2 + 2C_3 - a_L^2(B_2 + C_3) - a_T^2 (A_1 + C_3)]$$

$$+ i\omega\epsilon_0 [-A_1C_3 - B_2C_3 - A_3^2 + B_3^2 + 2\omega^2\epsilon_0^2 (1-a^2)] \tag{8}$$

$$a_1 = -2i\omega\epsilon_0 a_L (A_2A_3 + A_1B_3) - 2\omega^2\epsilon_0^2 a_L B_3(a^2 - 1) \tag{9}$$

$$a_0 = A_1B_2C_3 - 2A_2A_3B_3 + A_3^2B_2 - A_1B_3^2 + A_2^2C_3 + i\omega\epsilon_0(A_1C_3 + B_2C_3$$

$$+ A_1B_2 + A_2^2 + A_3^2 - B_3^2) - i\omega\epsilon_0 a_T^2 (A_1C_3 + A_1B_2 + A_3^2 + A_2^2)$$

$$+ i\omega\epsilon_0 a_L^2(-B_2C_3 - A_1B_2 + B_3^2 - A_2^2) - \omega^2\epsilon_0^2 (A_1 + B_2 + C_3)$$

$$+ \omega^2\epsilon_0^2 a_T^2(2A_1 + B_2 + C_3) + \omega^2\epsilon_0^2 a_L^2(A_1 + 2B_2 + C_3)$$

$$- \omega^2\epsilon_0^2 a_T^2 a_L^2 (A_1 + B_2) - \omega^2\epsilon_0^2 a_T^4 A_1 - \omega^2\epsilon_0^2 a_L^4 B_2 - i\omega^3\epsilon_0^3 (1-a^2)^2 . \tag{10}$$

The functions $\zeta_p(x)\left(p = \frac{5}{2}, \frac{3}{2}\right)$ can be evaluated by an application of quadrature techniques to the integrals [Johler and Walters, 1960], or other methods described by Dingle, and Roy [1956],

$$\xi_{5/2}(x) = \left(\frac{5}{2}!\right)\int_0^\infty \rho^{5/2}(x^2 + \rho^2)^{-1} \exp(-\rho)\, d\rho, \tag{11}$$

$$\xi_{3/2}(x) = \left(\frac{3}{2}!\right)\int_0^\infty \rho^{3/2}(x^2 + \rho^2)^{-1} \exp(-\rho)\, d\rho. \tag{12}$$

The quantities P and Q are rewritten[7];

$$P = \frac{-\left[a_L\zeta + \frac{B_3}{i\omega\epsilon_0}\right]\left[1 - a_L^2 - \zeta^2 + \frac{A_1}{i\omega\epsilon_0}\right] + \left[a_L a_T + \frac{A_2}{i\omega\epsilon_0}\right]\left[a_T\zeta - \frac{A_3}{i\omega\epsilon_0}\right]}{\left[1-a^2 + \frac{C_3}{i\omega\epsilon_0}\right]\left[1-a_L^2 - \zeta^2 + \frac{A_1}{i\omega\epsilon_0}\right] - \left[a_T\zeta + \frac{A_3}{i\omega\epsilon_0}\right]\left[a_T\zeta - \frac{A_3}{i\omega\epsilon_0}\right]} \tag{13}$$

$$Q = \frac{-\left[1 - a^2 + \frac{C_3}{i\omega\epsilon_0}\right]\left[a_L a_T + \frac{A_2}{i\omega\epsilon_0}\right] + \left[a_T\zeta + \frac{A_3}{i\omega\epsilon_0}\right]\left[a_L\zeta + \frac{B_3}{i\omega\epsilon_0}\right]}{\left[1 - a^2 + \frac{C_3}{i\omega\epsilon_0}\right]\left[1-a_L^2 - \zeta^2 + \frac{A_1}{i\omega\epsilon_o}\right] - \left[a_T\zeta - \frac{A_3}{i\omega\epsilon_0}\right]\left[a_T\zeta \frac{A_3}{i\omega\epsilon_0}\right]}. \tag{14}$$

[7] The constant ϵ_0 or the factor $i\omega\epsilon_0$ can be eliminated from eq (1 - 3, 6 - 10, 13 and 14) for convenience. The factor was retained so that eq (37), would be correct dimensionally, ie., J = current, amperes per square meter.

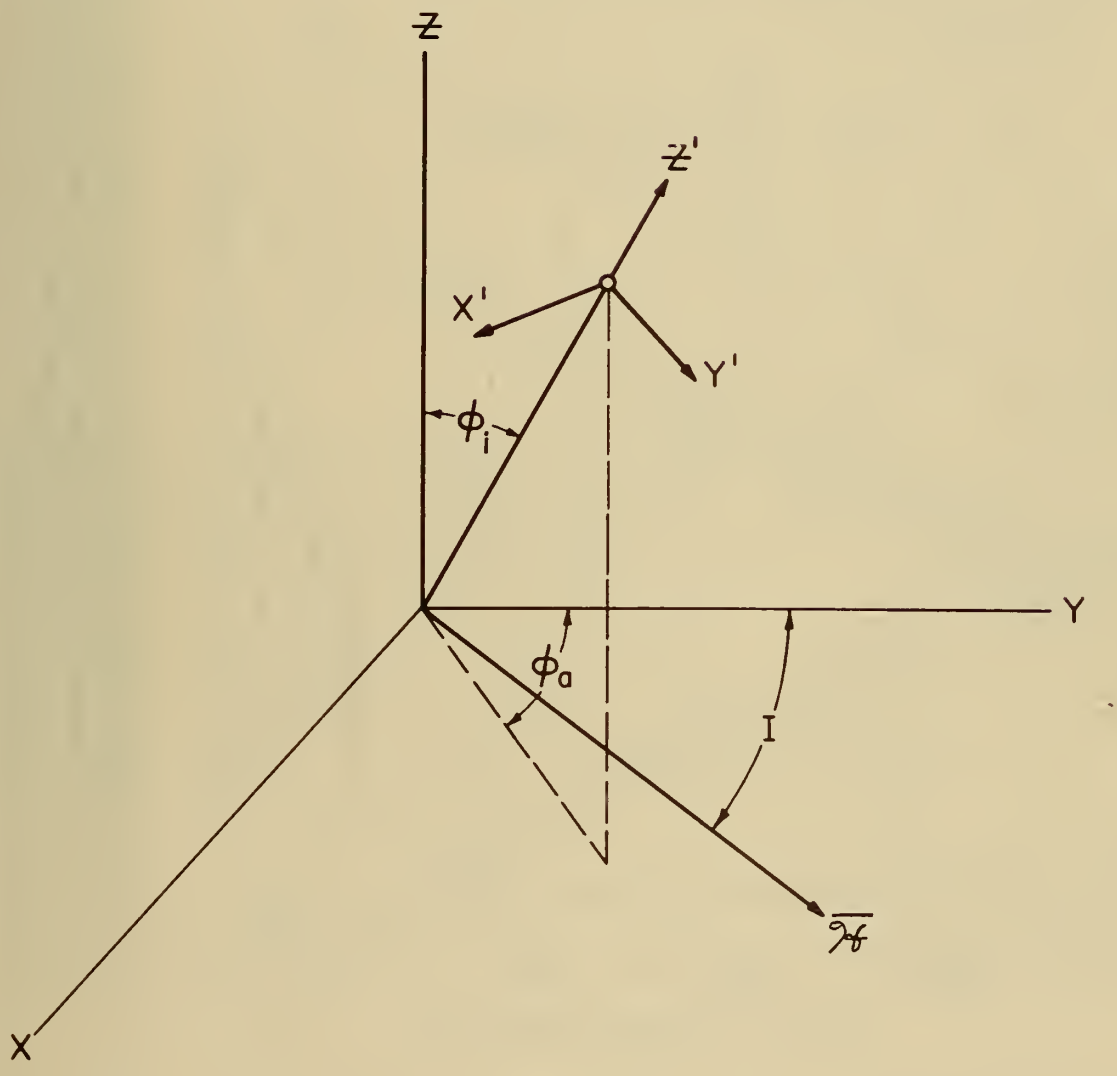

Fig. 1 - Coordinate systems, illustrating angle of incidence, ϕ_i, magnetic azimuth, ϕ_a, magnetic dip, I, of the magnetic field.

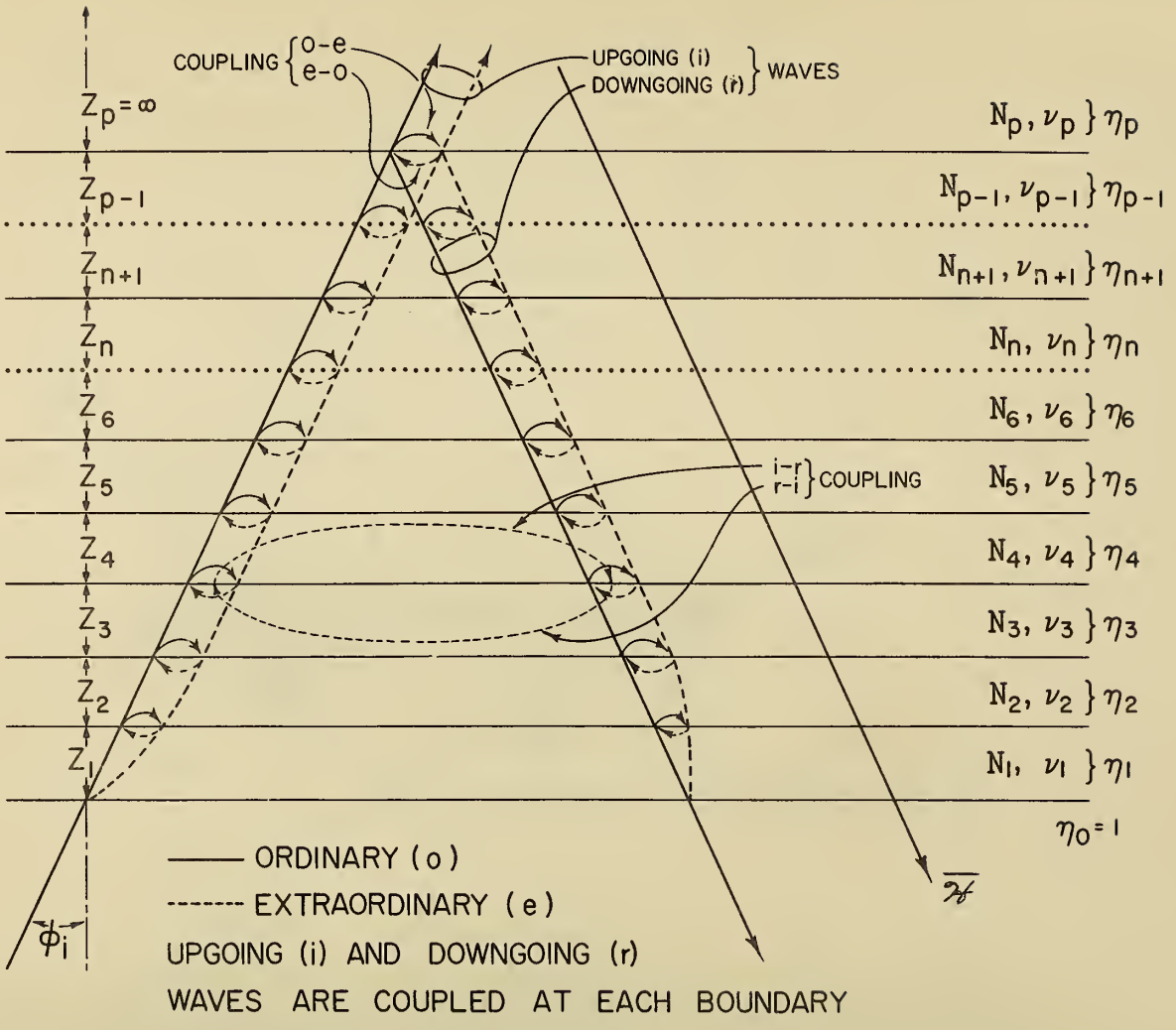

Fig. 2 - Structure of continuously stratified plasma model illustrating ordinary (o) and extraordinary (e), upgoing (i) and downgoing (r) propagation components coupled at each boundary. Each Z_n, n=1, 2, 3... p, becomes smaller as the number of slabs or stratum, p, is increased until a stable reflection or transmission is obtained.

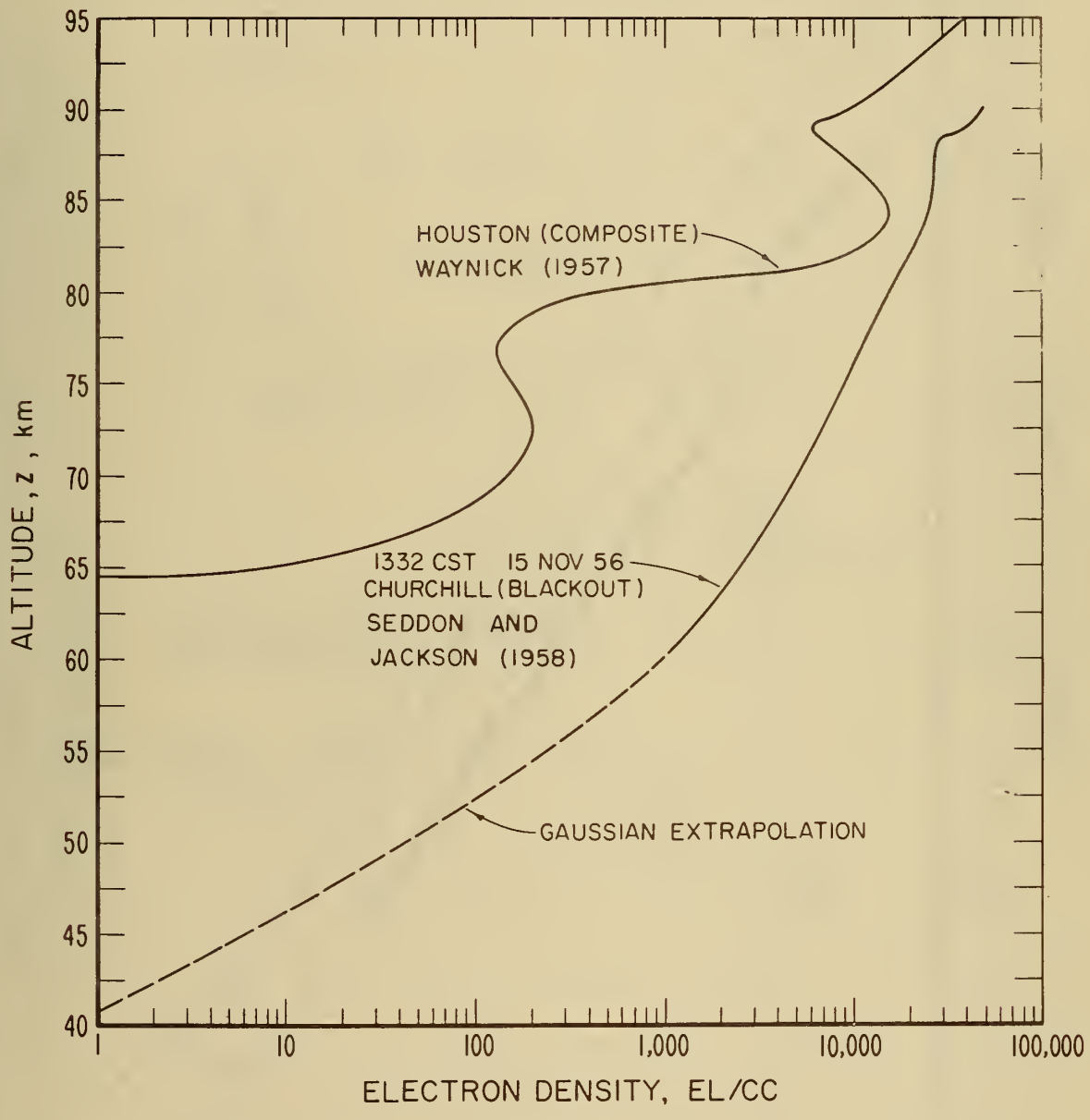

Fig. 3 - Electron density-altitude N(z), profiles of the lower ionosphere illustrating approximate daytime-noon (Houston) and local ionosonde blackout conditions.

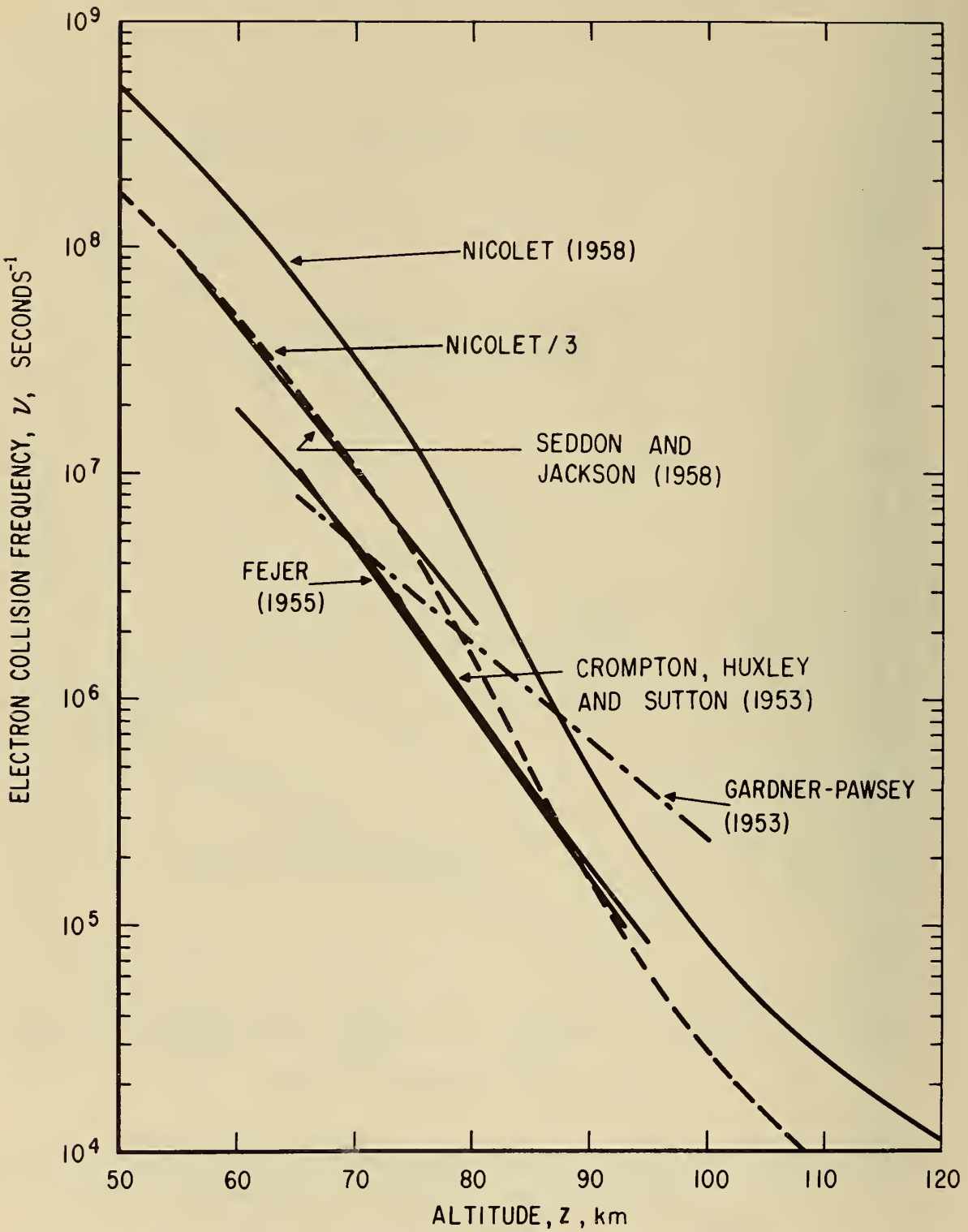

Fig. 4 - Collision frequency-altitude, $\nu(z)$, profiles of the lower ionosphere, illustrating various estimates of the classical collision frequency

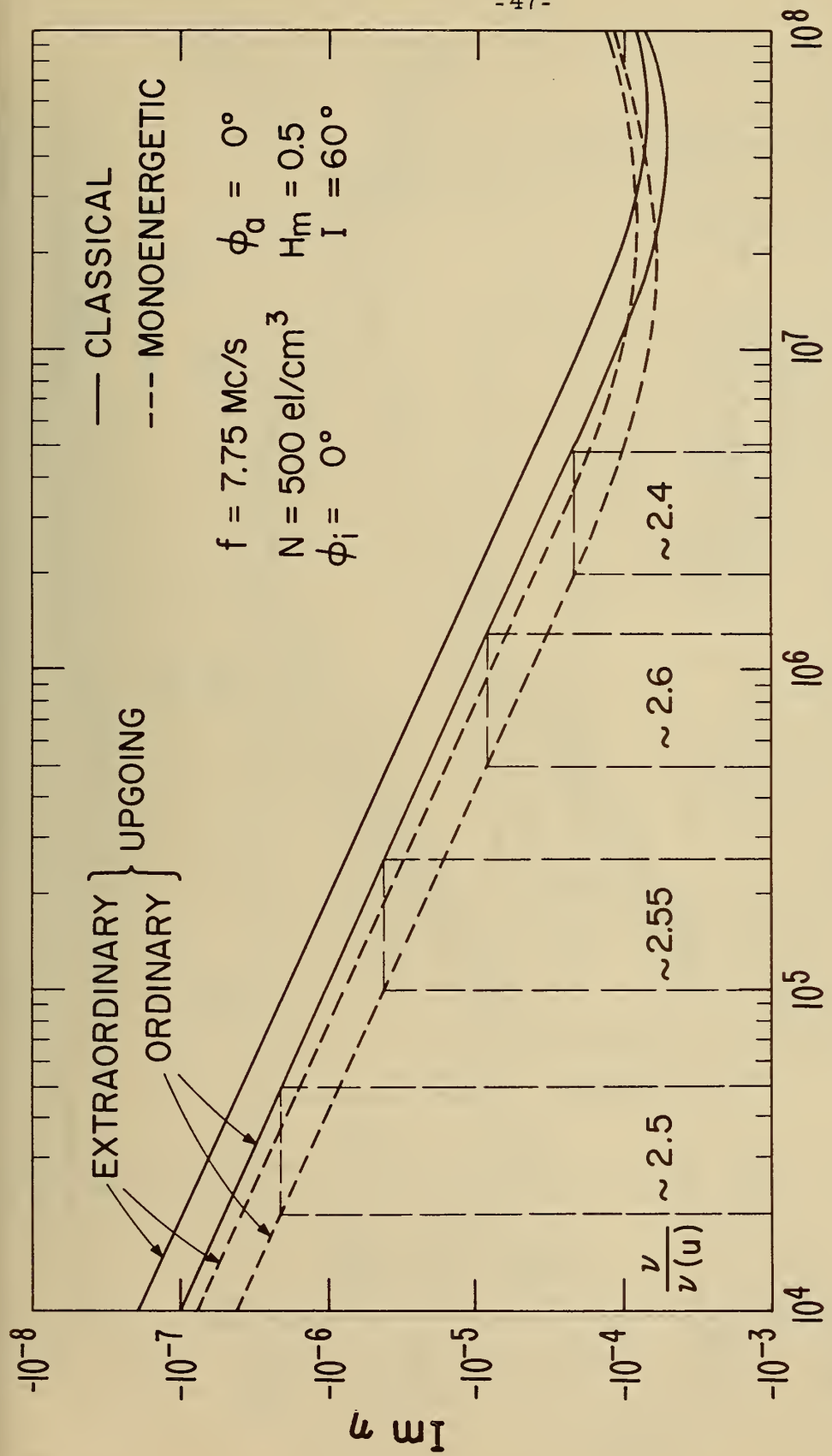

Fig. 5 - Comparison of imaginary part of complex index of refraction, $\mathrm{Im}\,\eta_{o,e}$, for classical and monoenergetic magneto-ionic theories at 7.75 megacycles, illustrating theoretical basis for the ratio $\nu/\nu(u) \sim 2.5$ (Kane [1960] made measurements of $\nu(u)$ at a frequency f = 7.75 Mc/s).

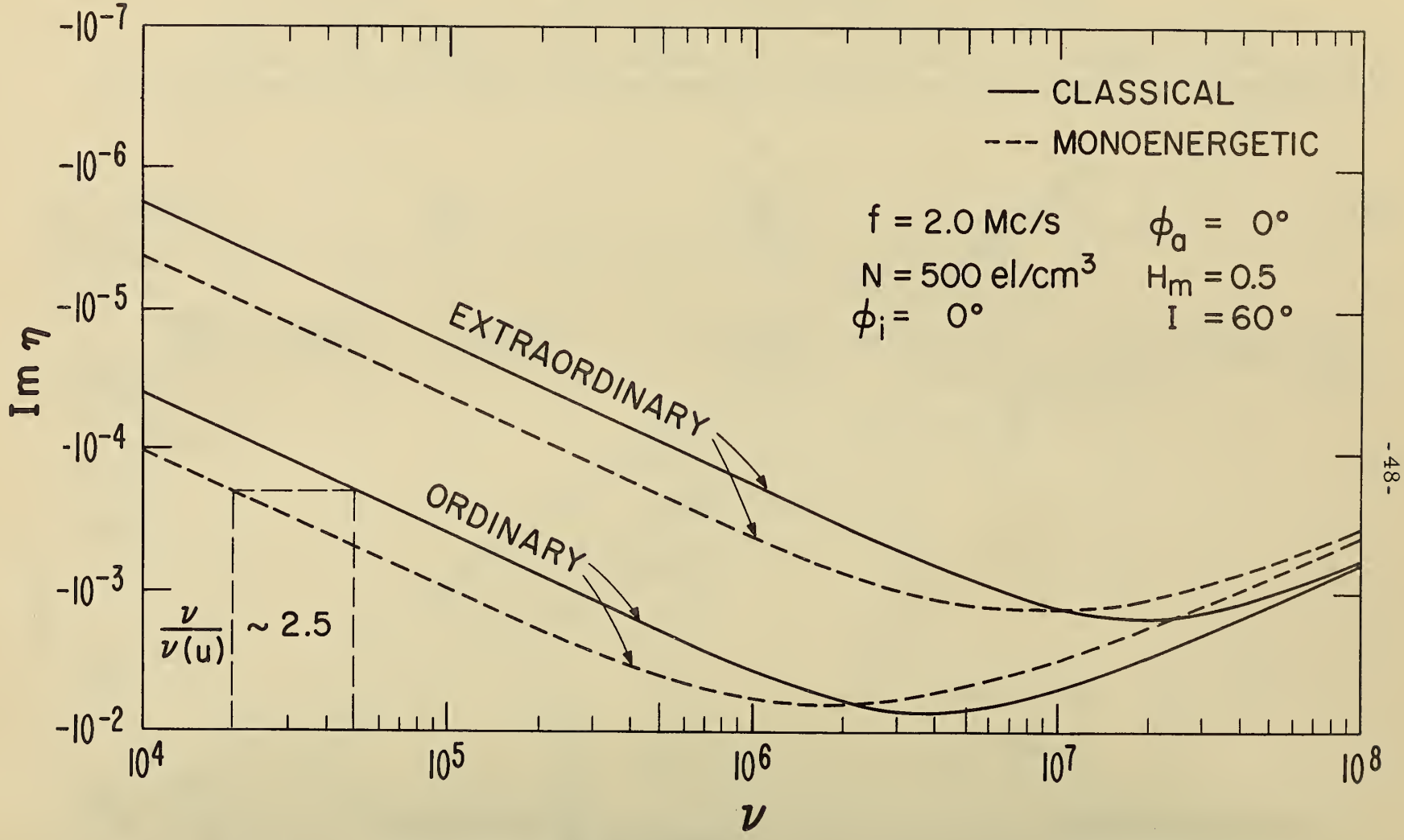

Fig. 6 - Comparison of imaginary part of complex index of refraction, $\mathrm{Im}\eta_{o,e}$, for classical and monoenergetic magneto-ionic theories at 2.0 Megacycles, illustrating theoretical basis for ratio $\nu/\nu(u) \sim 2.5$.

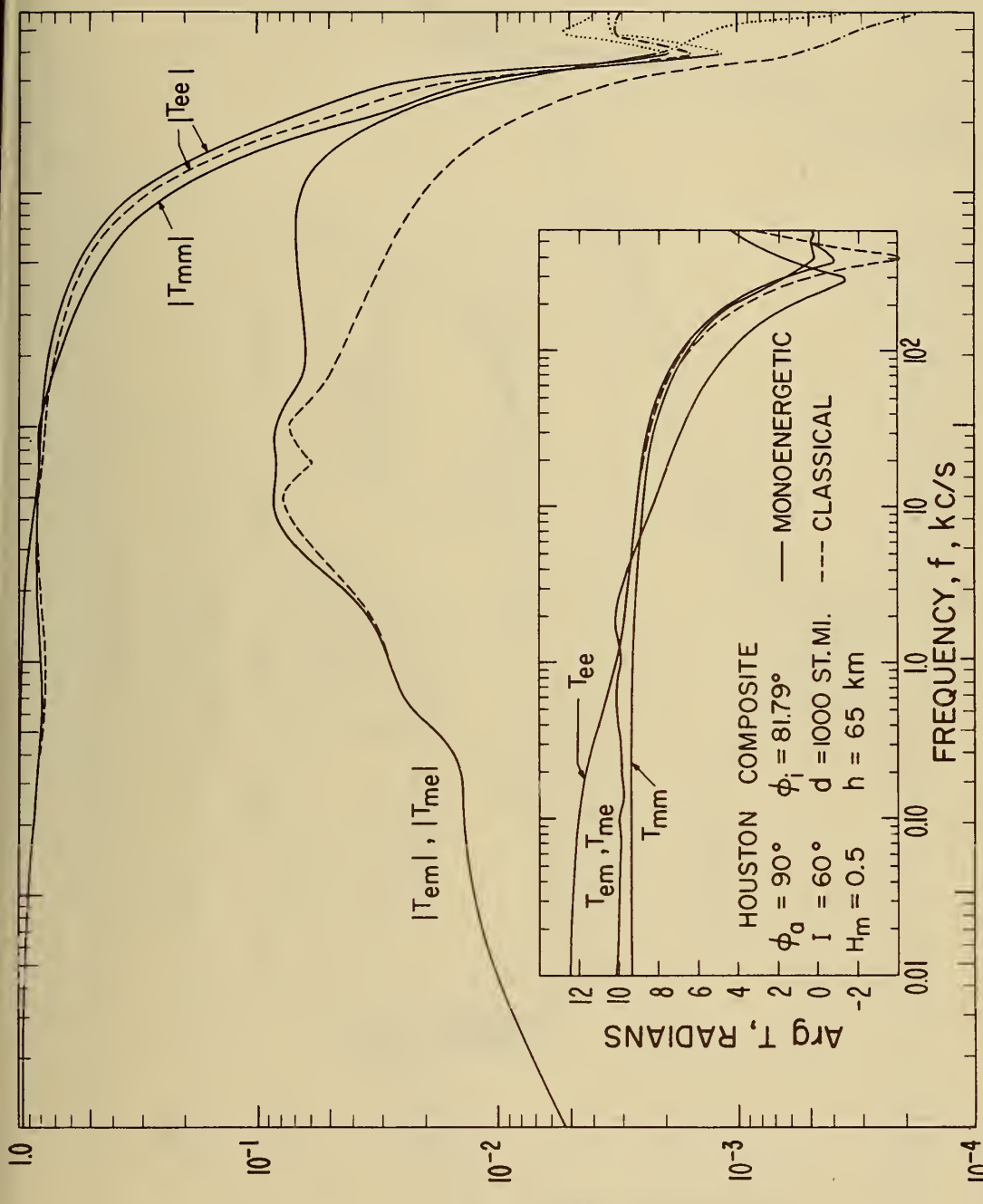

Fig. 7 - Amplitude, |T|, and phase, arg T, of the reflection coefficient, T, as a function of frequency (f = 10 c/s to 600 kc/s), illustrating a comparison of the amplitude for classical and monoenergetic theories, for propagation into the east, $\phi_a = 90^o$.

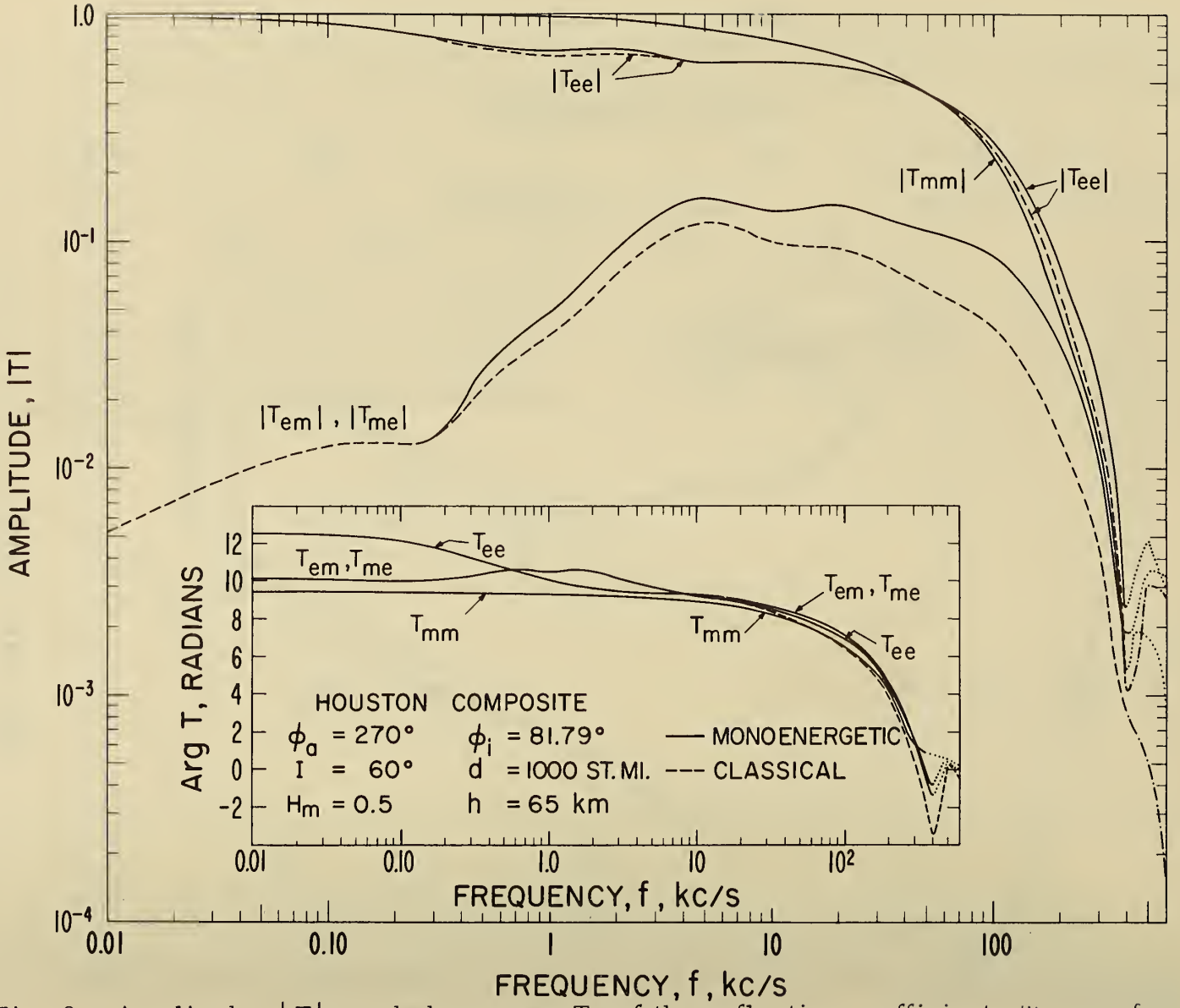

Fig. 8 - Amplitude, $|T|$, and phase, arg T, of the reflection coefficient, T, as a function of frequency (f = 10 c/s to 600 kc/s), illustrating a comparison of the amplitude for classical and monoenergetic theories, for propagation into the west, $\phi_a = 270^{\circ}$.

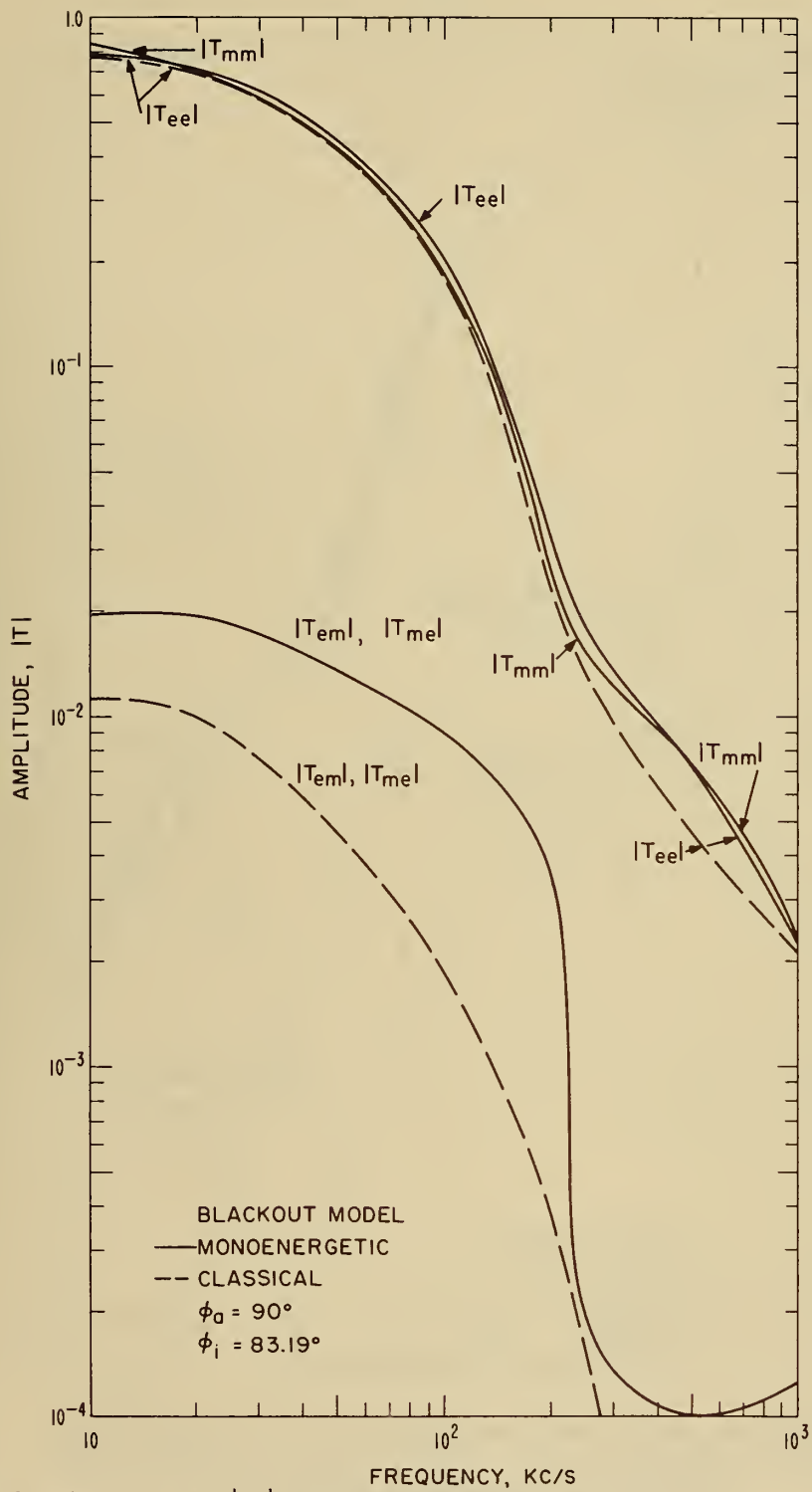

Fig. 9 - Amplitude, $|T|$, of the reflection coefficient, T, as a function of frequency (f = 10 kc/s to 1 Mc/s) illustrating a comparison of the amplitude for classical and monoenergetic theories, for propagation into the east, ϕ_a = 90°.

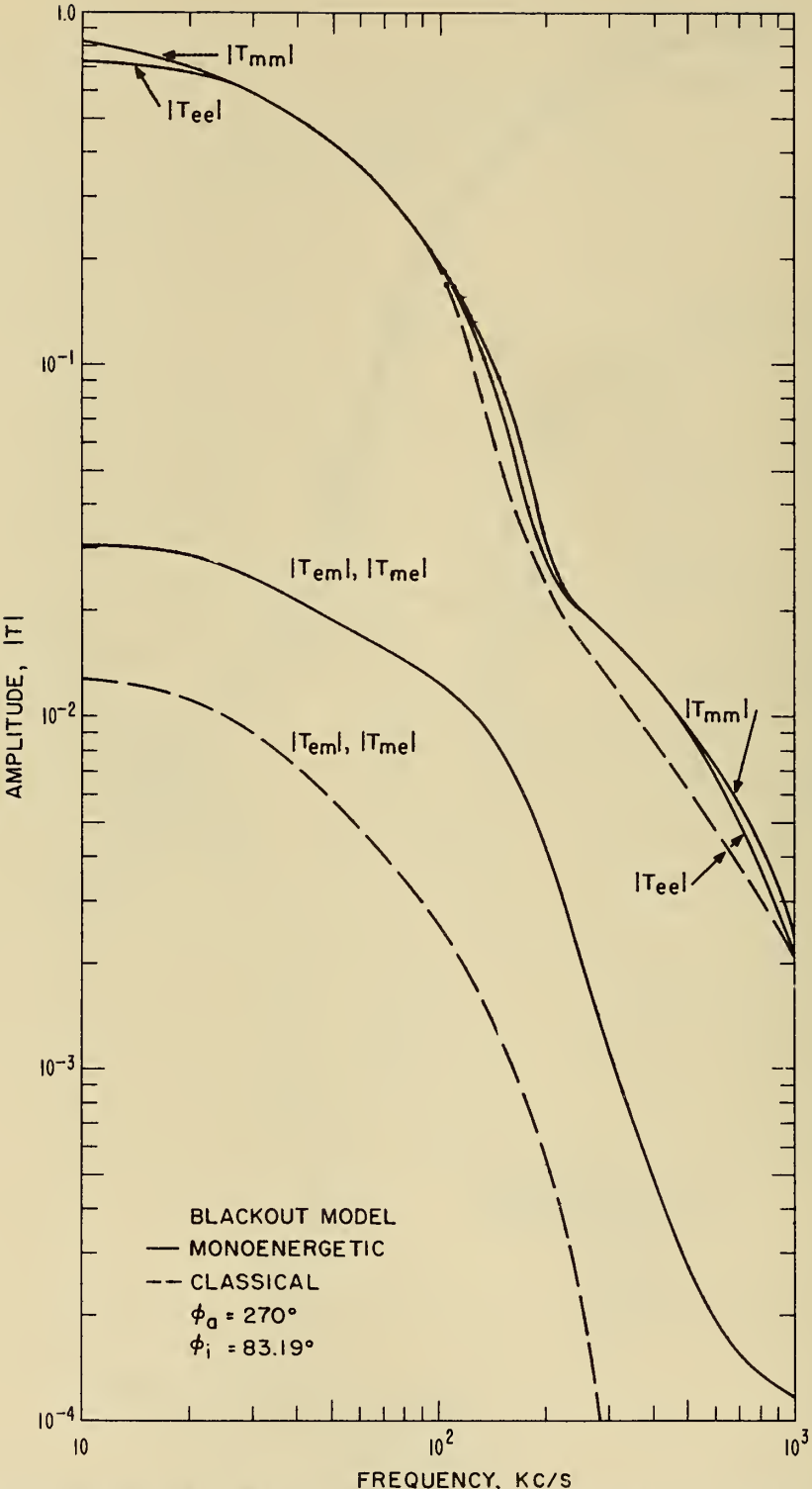

Fig. 10 - Amplitude, $|T|$, of the reflection coefficient, T, as a function of frequency (f = 10 kc/ s to 1 Mc/ s) illustrating a comparison of the amplitude for classical and monoenergetic theories, for propagation into the west, $\phi_a = 270°$.

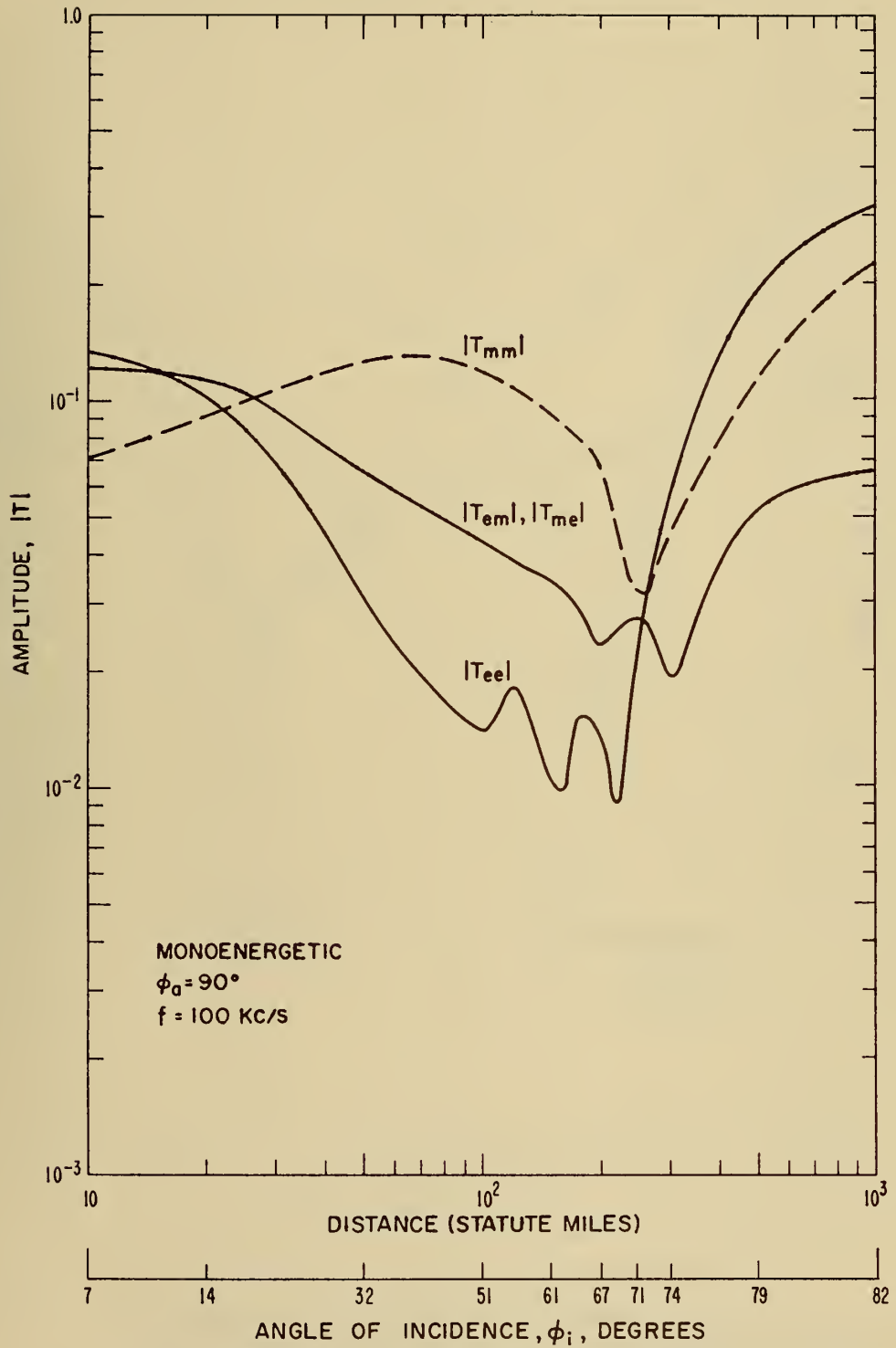

Fig. 11 - Amplitude, $|T|$, of the reflection coefficient, T, as a function of angle of incidence, ϕ_i, for propagation into the east, $\phi_a = 90°$ based on monoenergetic collision frequencies.

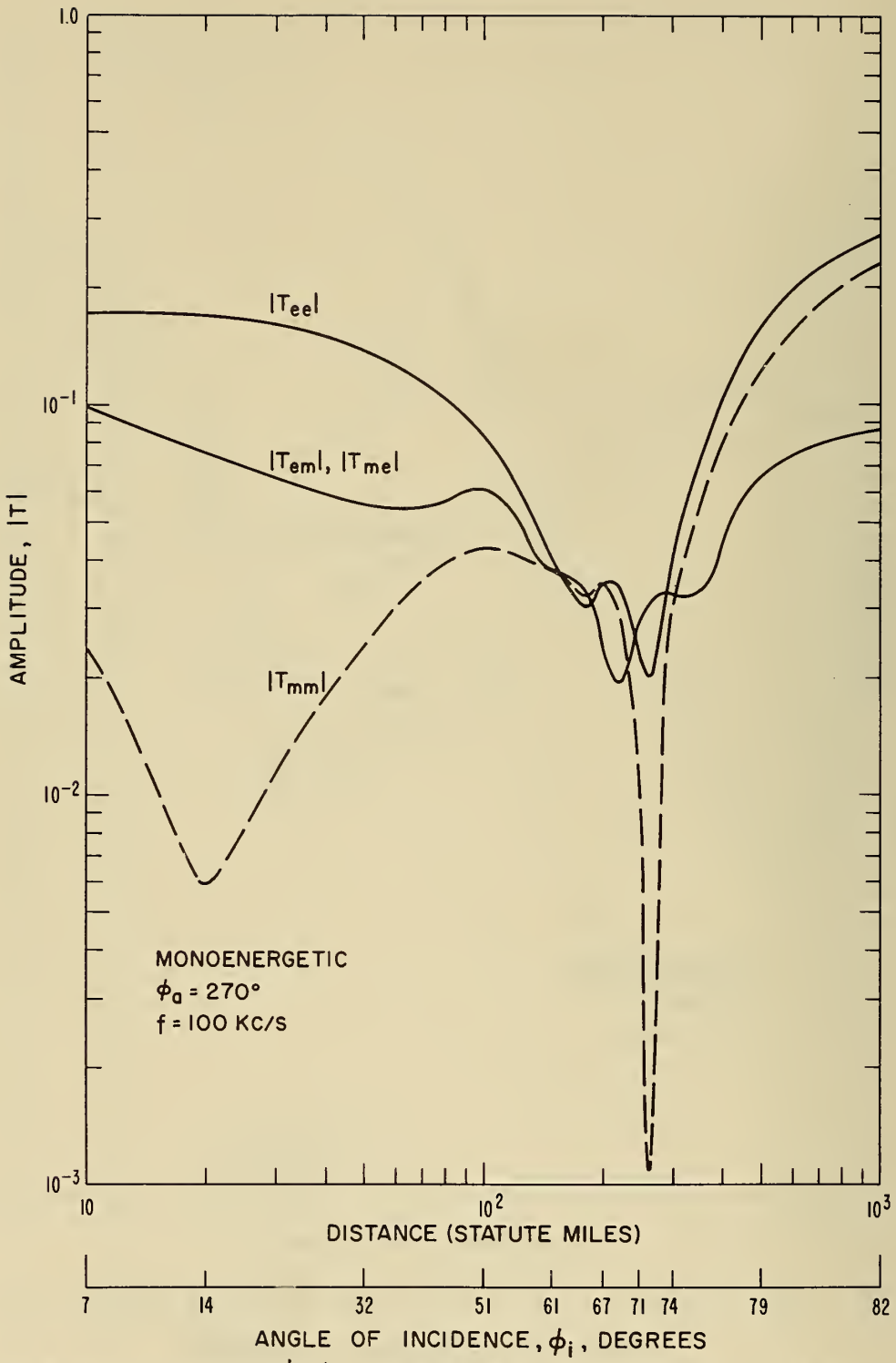

Fig. 12 - Amplitude, $|T|$, of the reflection coefficient, T, as a function of angle of incidence, ϕ_i, for propagation into the west, ϕ_a = 270, based on monoenergetic collision frequencies.

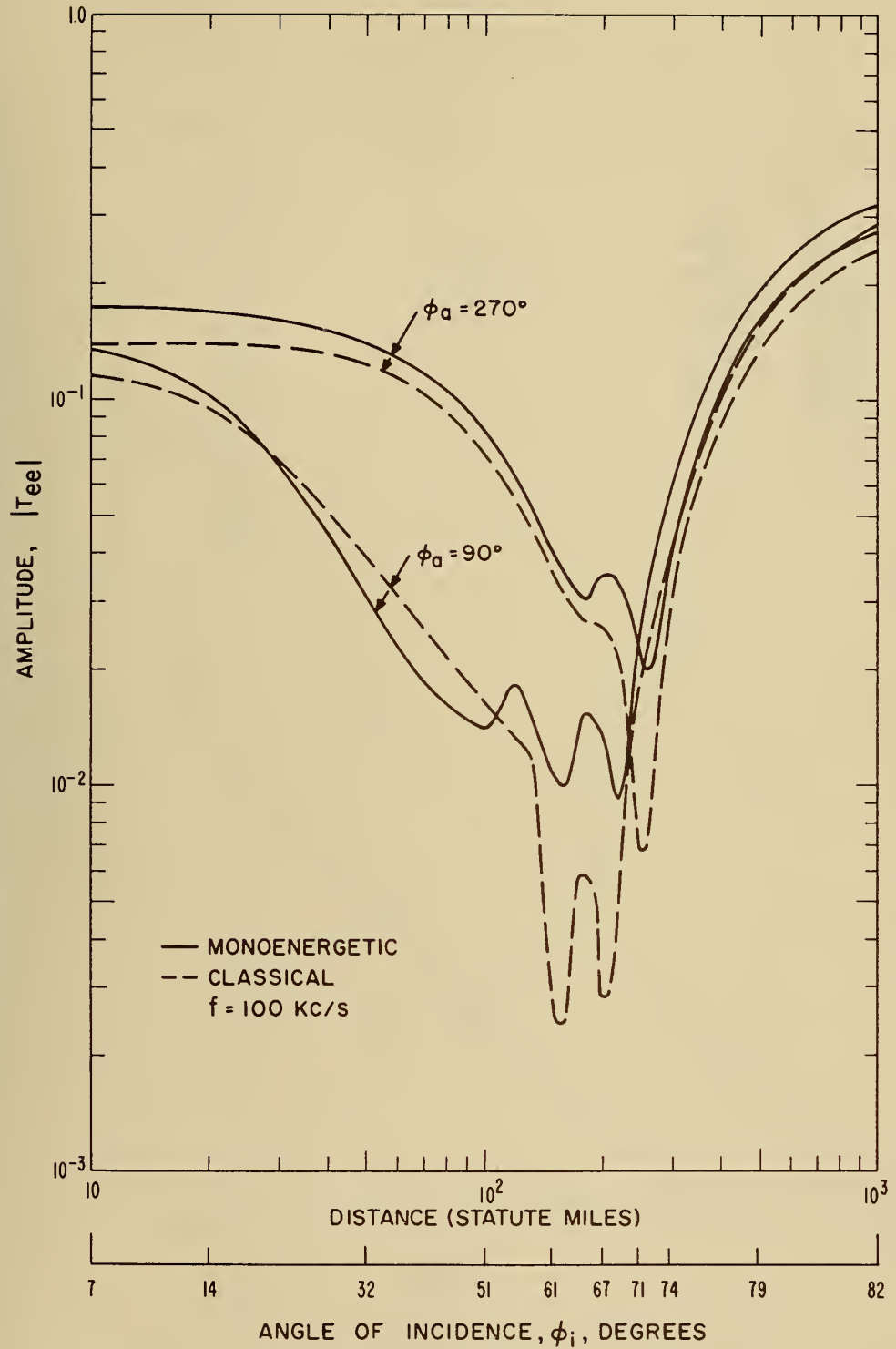

Fig. 13 - Comparison of the amplitude $|T_{ee}|$ of the reflection coefficient for vertical polarization based on the classical constant collision frequency with the same reflection coefficient based on electron collisions proportional to energy (monoenergetic) as a function of angle of incidence, ϕ_i, for propagation into the east $\phi_a = 90^o$ and propagation into the west, $\phi_a = 270^o$.

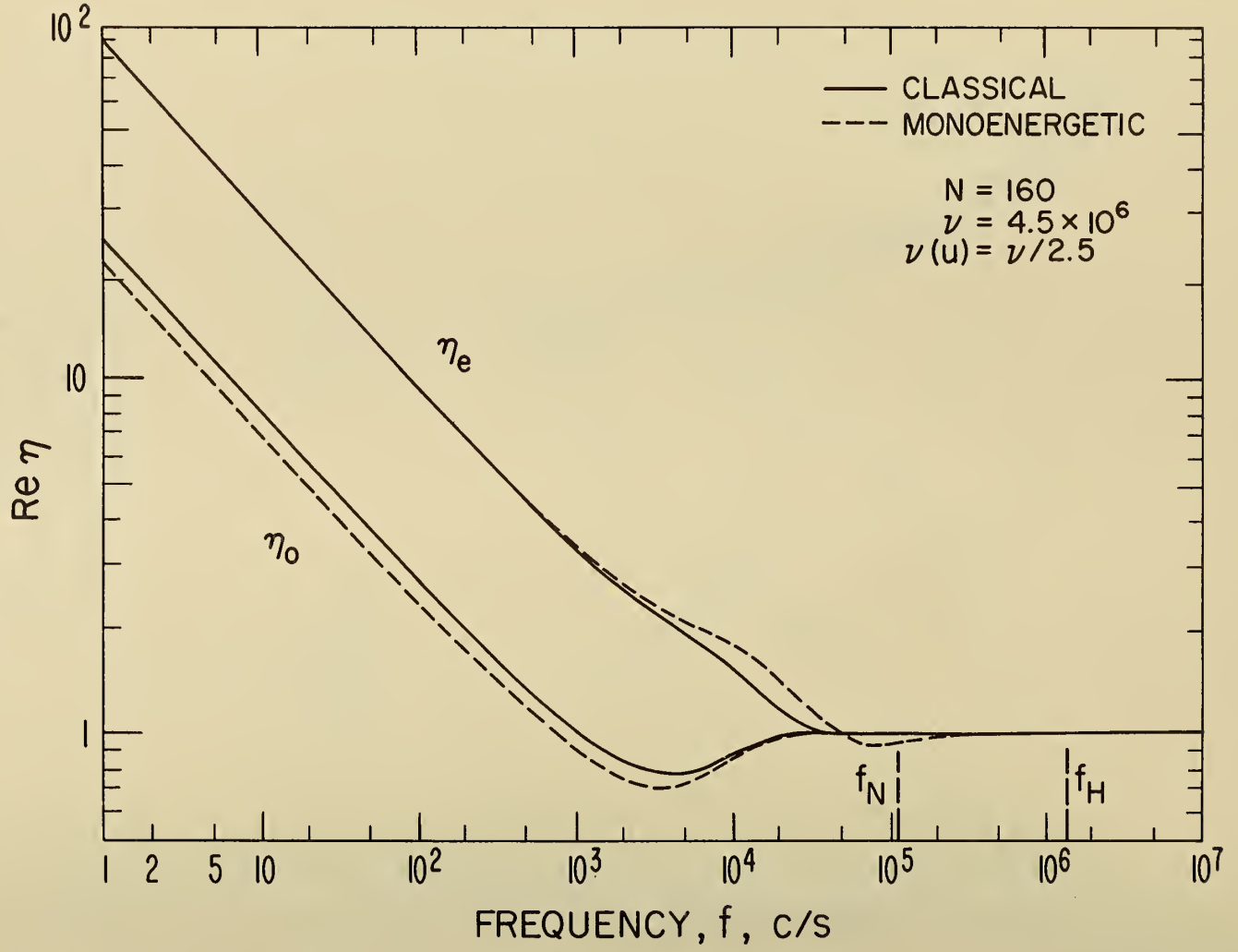

Fig. 14 - Real part of complex index of refraction, Re η, of the lower ionosphere for upgoing ordinary (o) and extraordinary (e), propagation components, illustrating the comparison of values based on the classical magneto-ionic theory with those based on the monoenergetic theory.

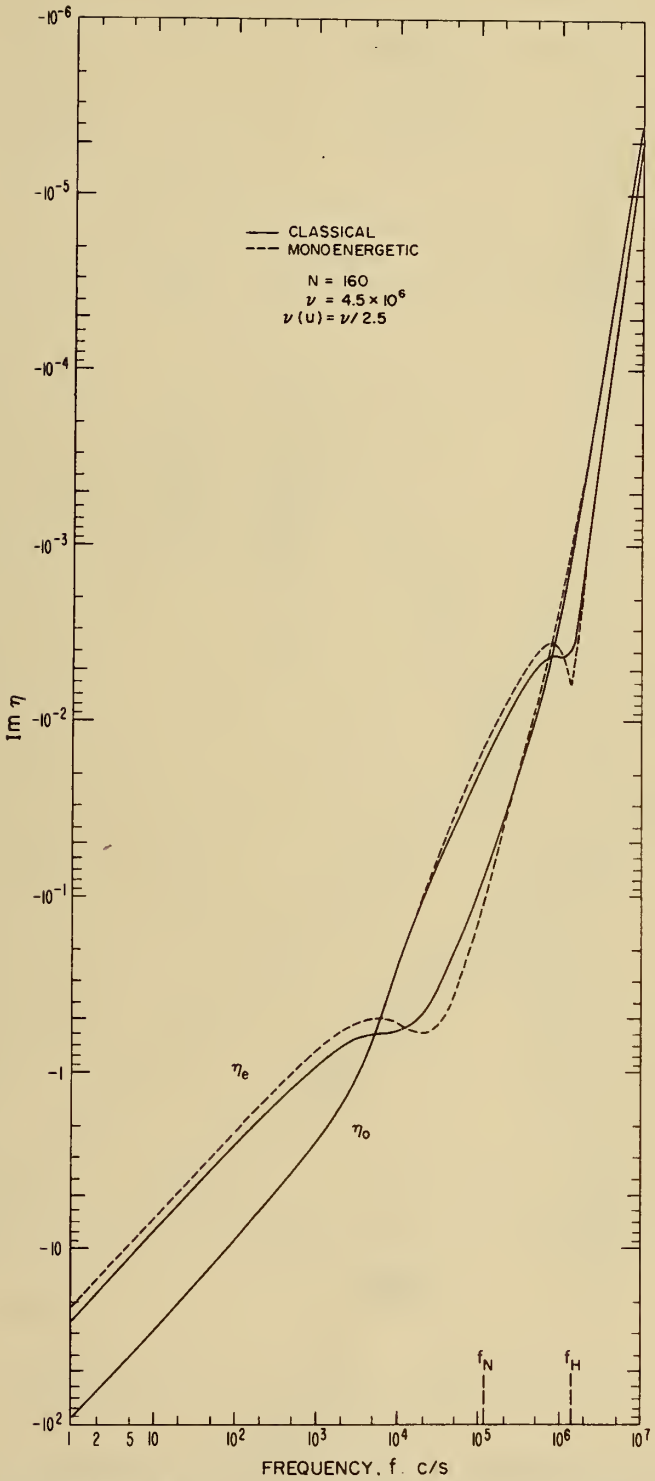

Fig. 15 - Imaginary part of complex index of refraction, Im η, of the lower ionosphere for upgoing ordinary (o) and extraordinary (e), propagation components, illustrating the comparison of values based on the classical magnetoionic theory with those based on the monoenergetic theory.

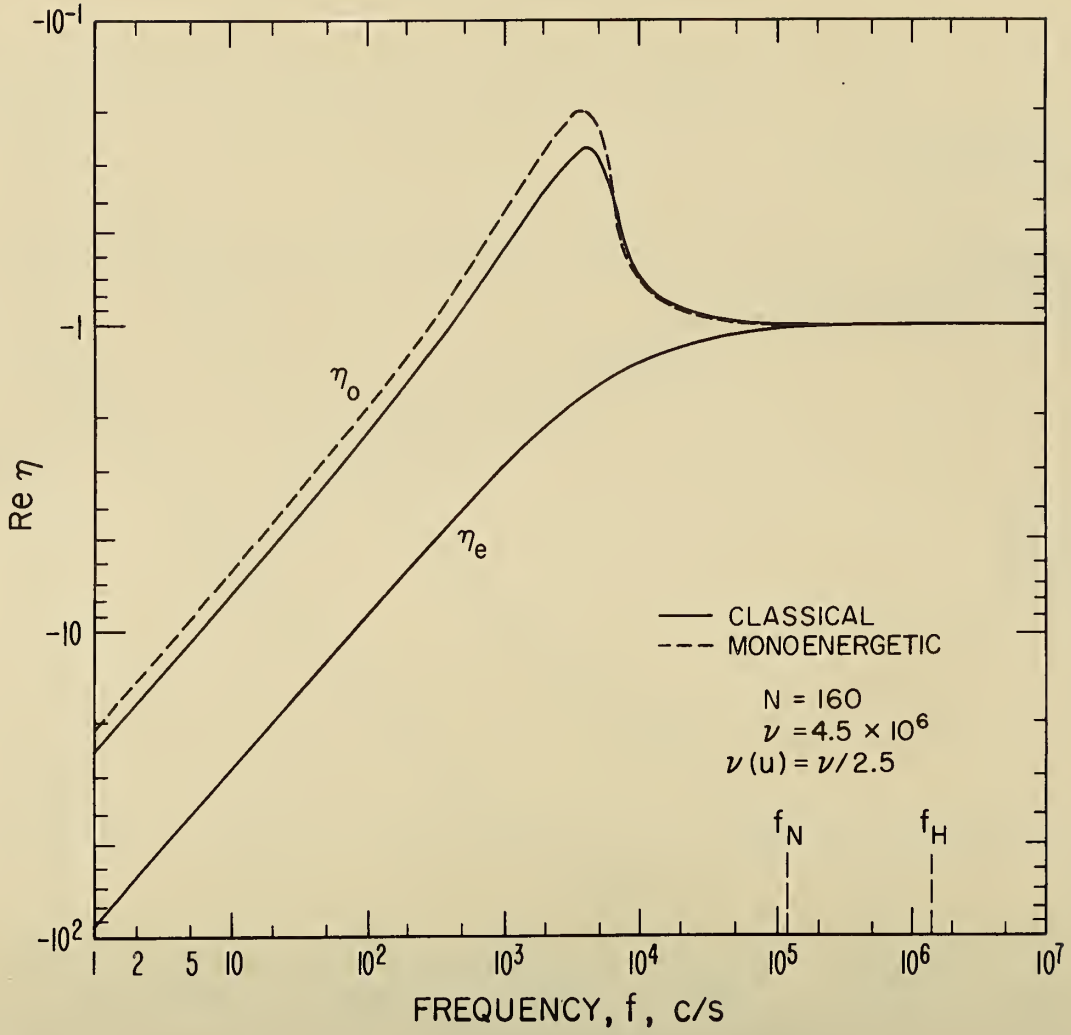

Fig. 16 - Real part of complex index of refraction, Re η, of the lower ionosphere for upgoing ordinary (o) and extraordinary (e), propagation components, illustrating the comparison of values based on the classical magneto-ionic theory with those based on the monoenergetic theory.

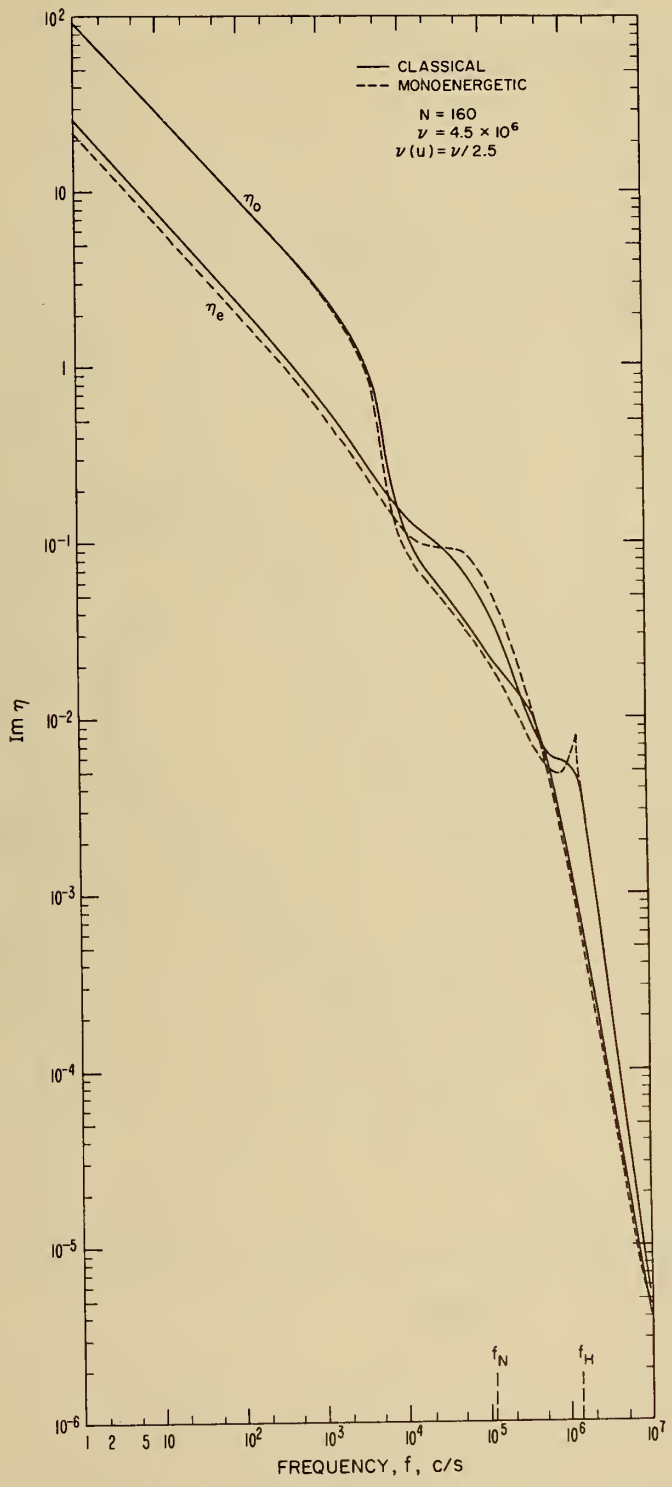

Fig. 17 - Imaginary part of complex index of refraction, Im η, of the lower ionosphere for upgoing ordinary (o) and extraordinary (e), propagation components, illustrating the comparison of values based on the classical magneto-ionic theory with those based on the monoenergetic theory.

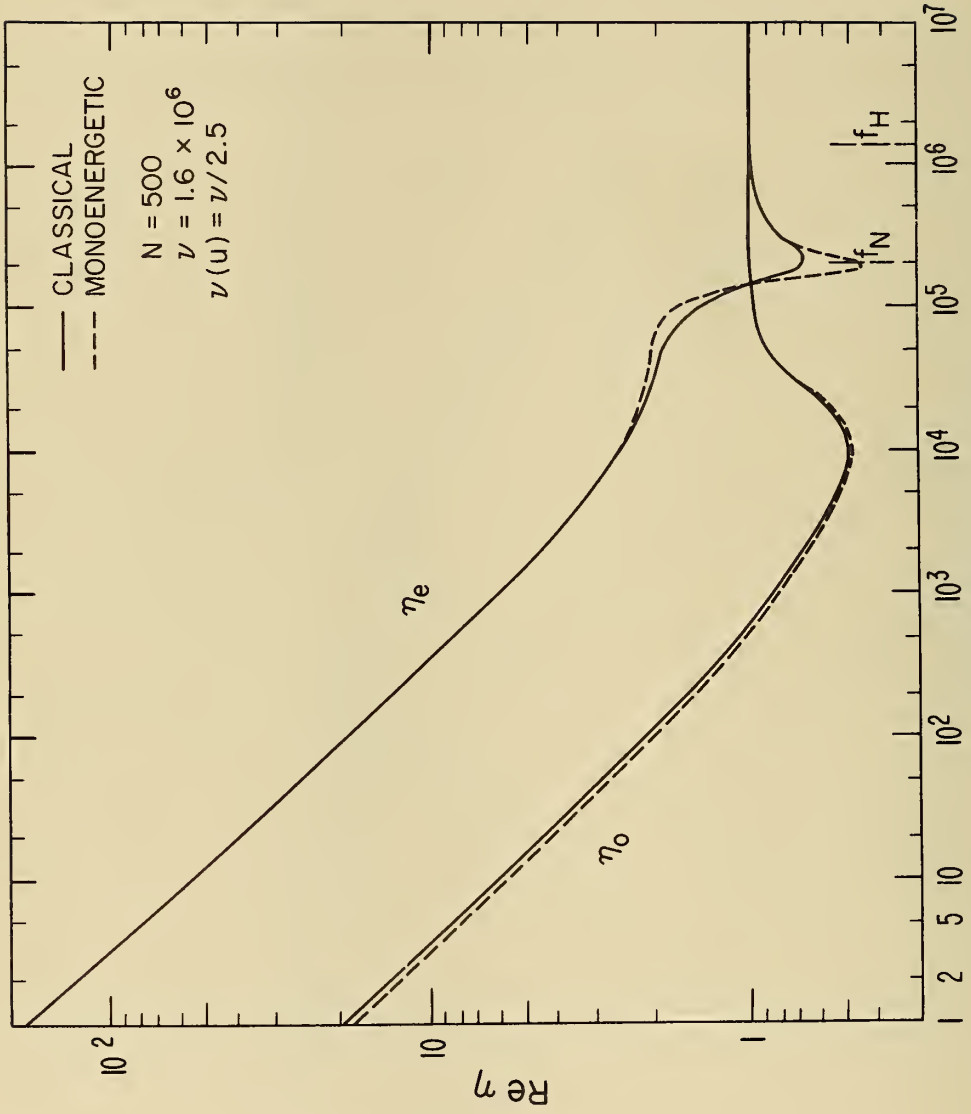

Fig. 18 - Real part of complex index of refraction, Re η, of the lower ionosphere for upgoing ordinary (o) and extraordinary (e), propagation components, illustrating the comparison of values based on the classical magneto-ionic theory with those based on the monoenergetic theory.

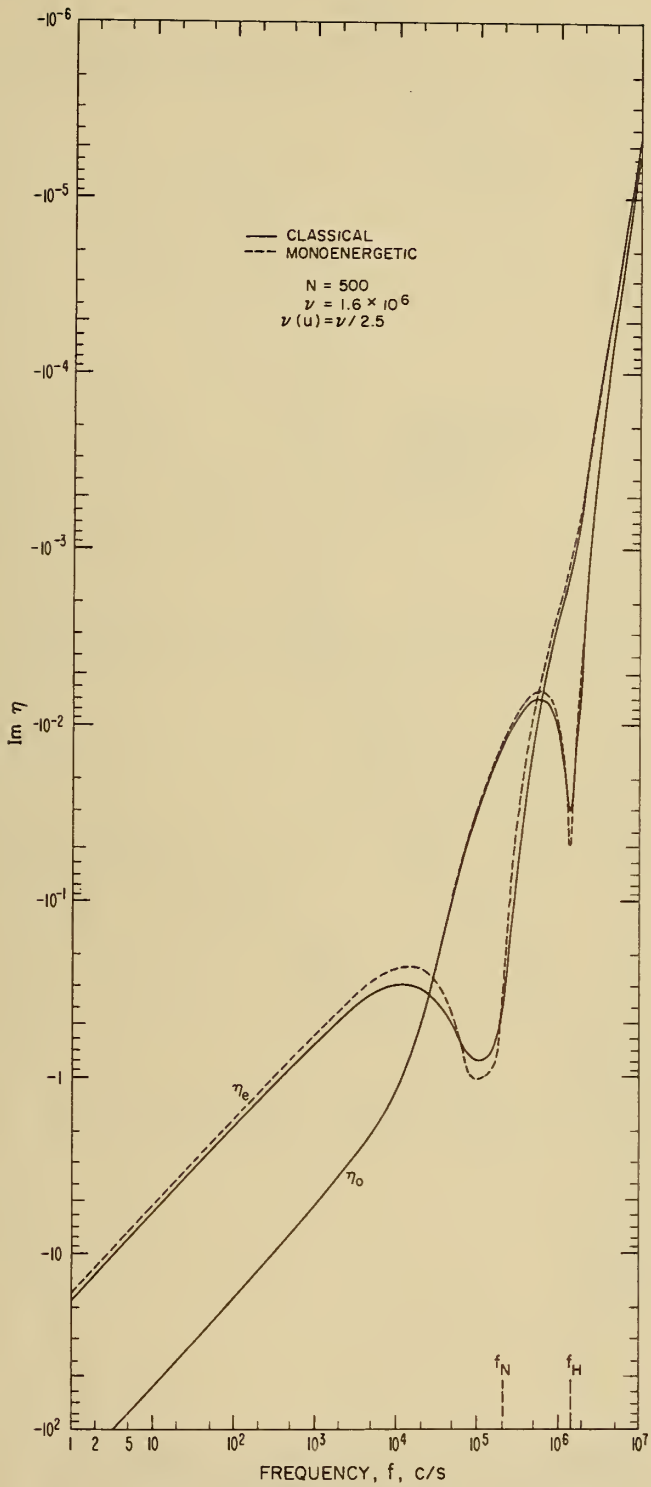

Fig. 19 - Imaginary part of complex index of refraction, Im η, of the lower ionosphere for upgoing ordinary (o) and extraordinary (e), propagation components, illustrating the comparison of values based on the classical magneto-ionic theory with those based on the monoenergetic theory.

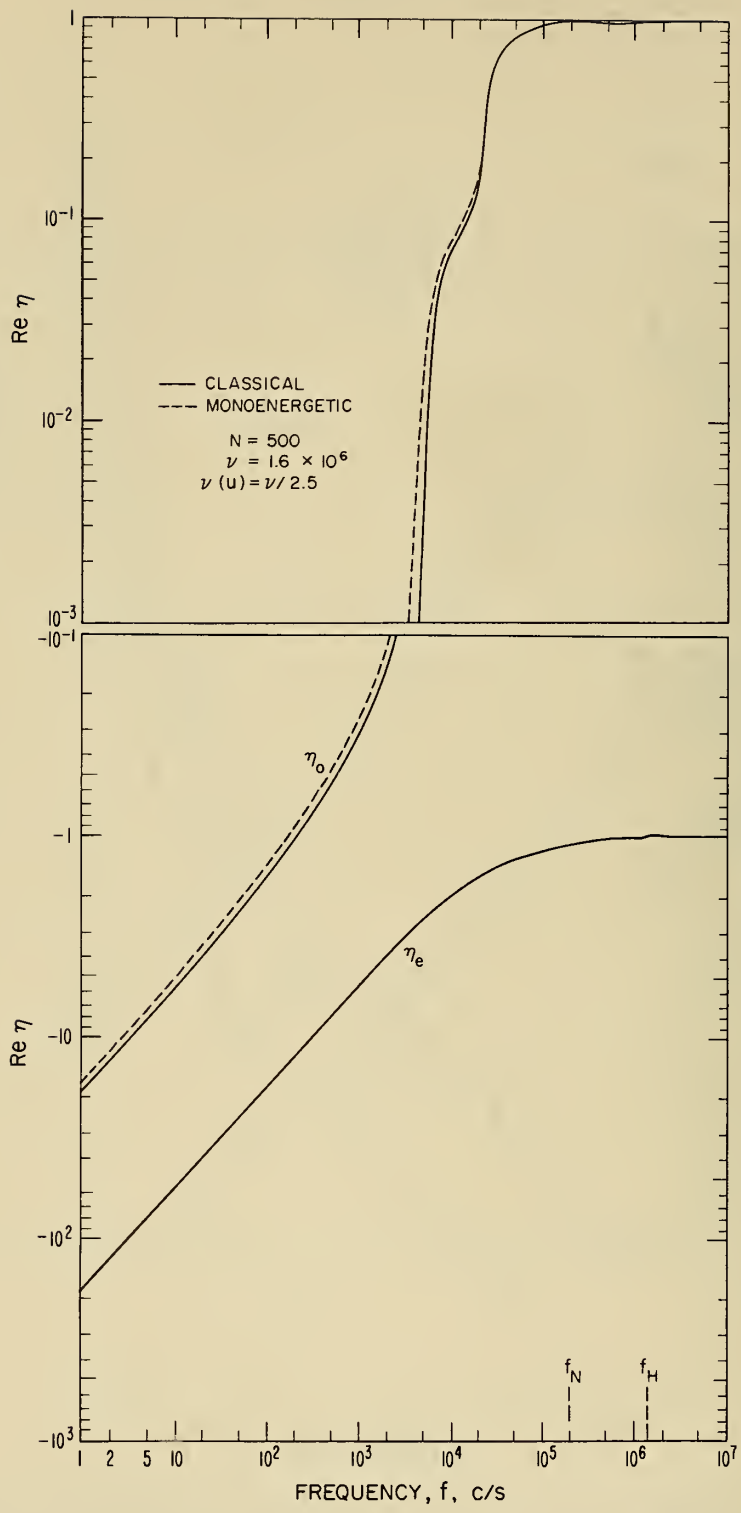

Fig. 20. Real part of complex index of refraction, Re η, of the lower ionosphere for upgoing ordinary (o) and extraordinary (e), propagation components, illustrating the comparison of values based on the classical magneto-ionic theory with those based on the monoenergetic theory.

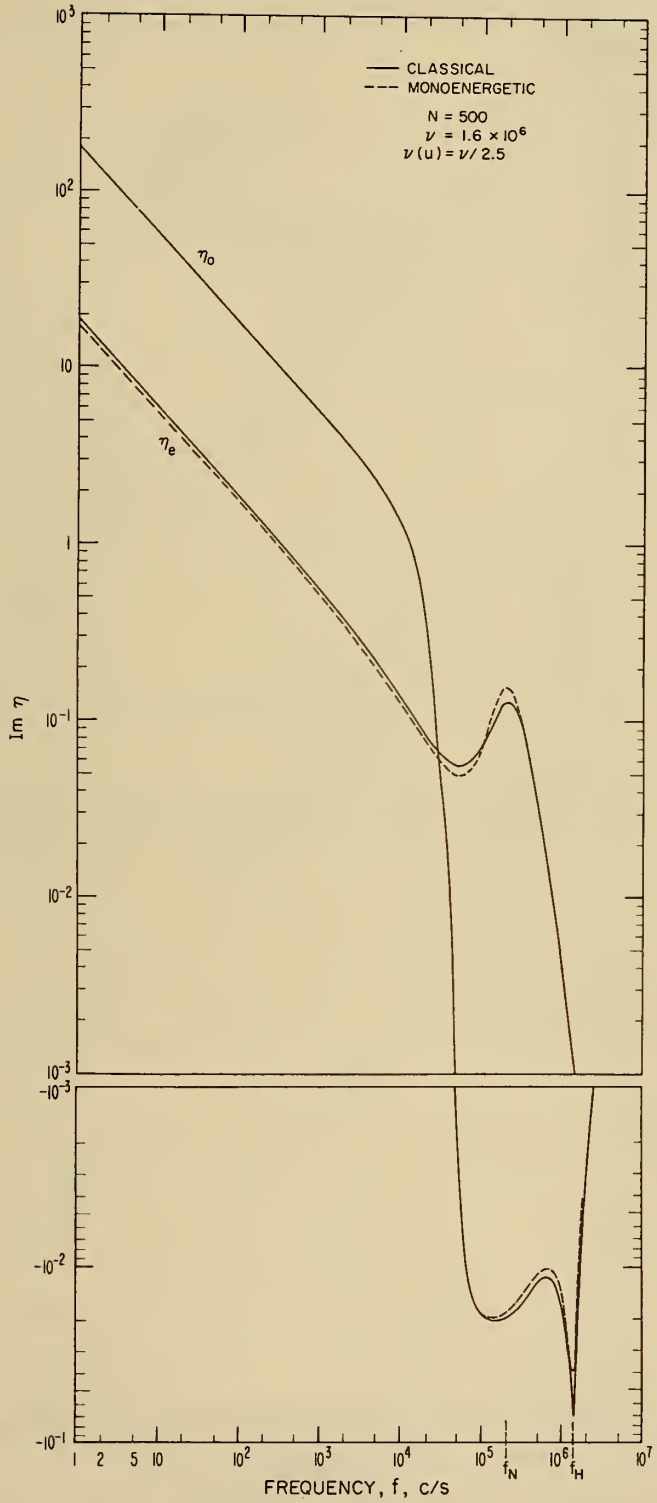

Fig. 21. Imaginary part of complex index of refraction, Im η, of the lower ionosphere for upgoing ordinary (o) and extraordinary (e), propagation components, illustrating the comparison of values based on the classical magneto-ionic theory with those based on the monoenergetic theory.

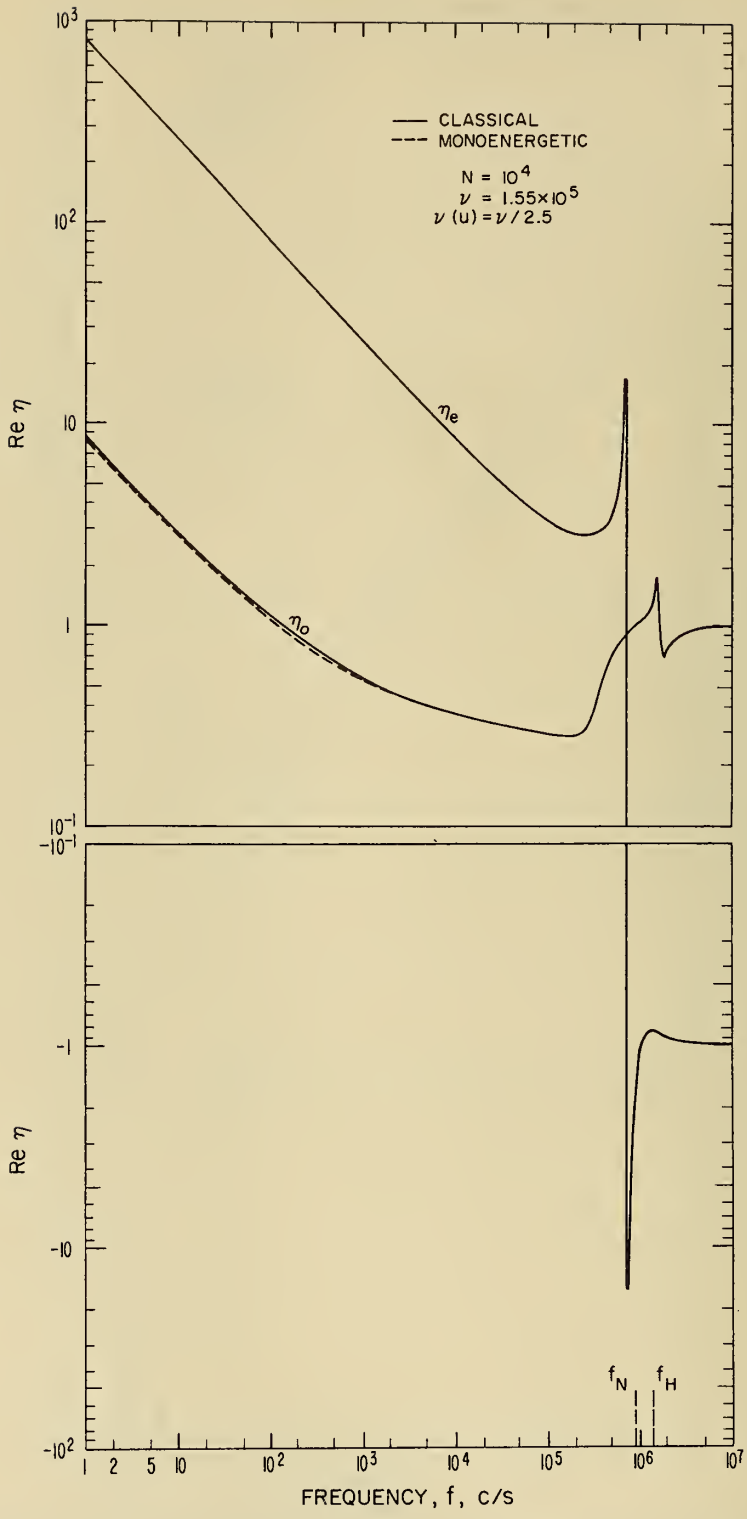

Fig. 22. Real part of complex index of refraction, Re η, of the lower ionosphere for upgoing ordinary (o) and extraordinary (e), propagation components, illustrating the comparison of values based on the classical magneto-ionic theory with those based on the monoenergetic theory.

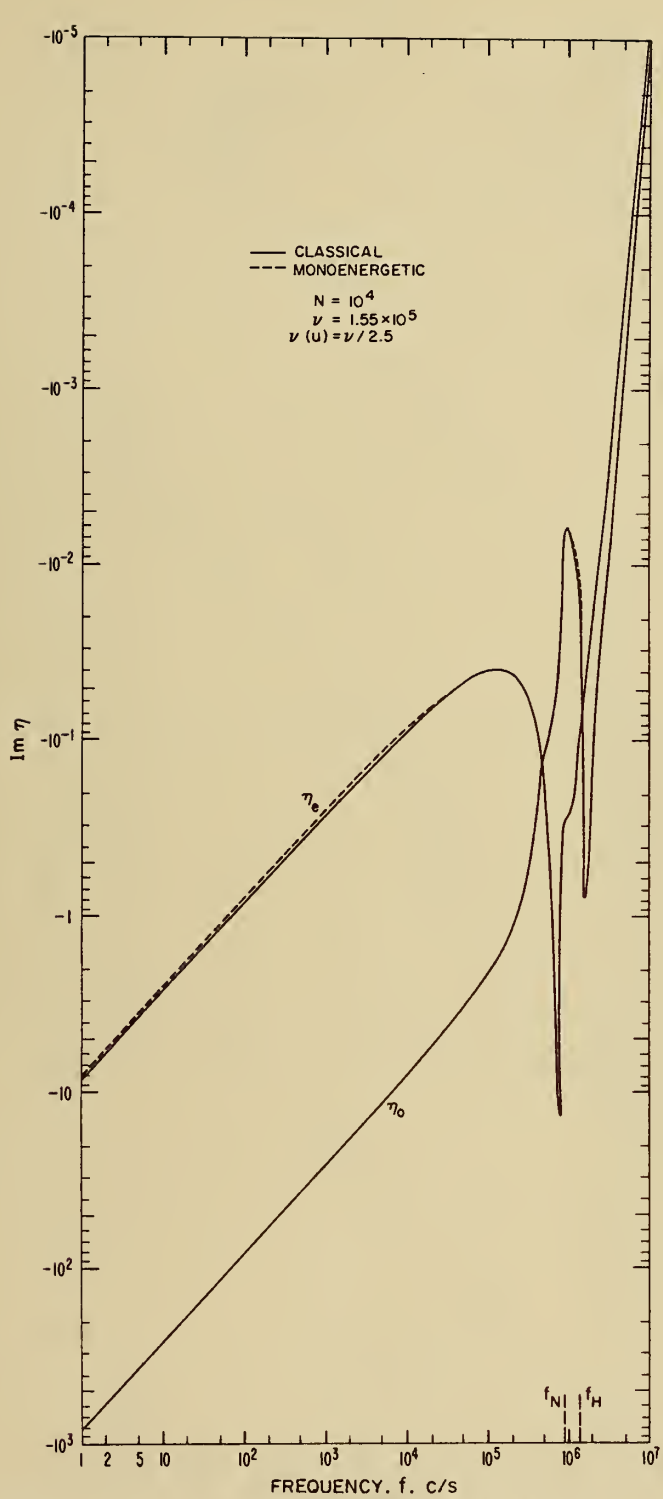

Fig. 23 - Imaginary part of complex index of refraction, Im η, of the lower ionosphere for upgoing ordinary (o) and extraordinary (e), propagation components, illustrating the comparison of values based on the classical magneto-ionic theory with those based on the monoenergetic theory.

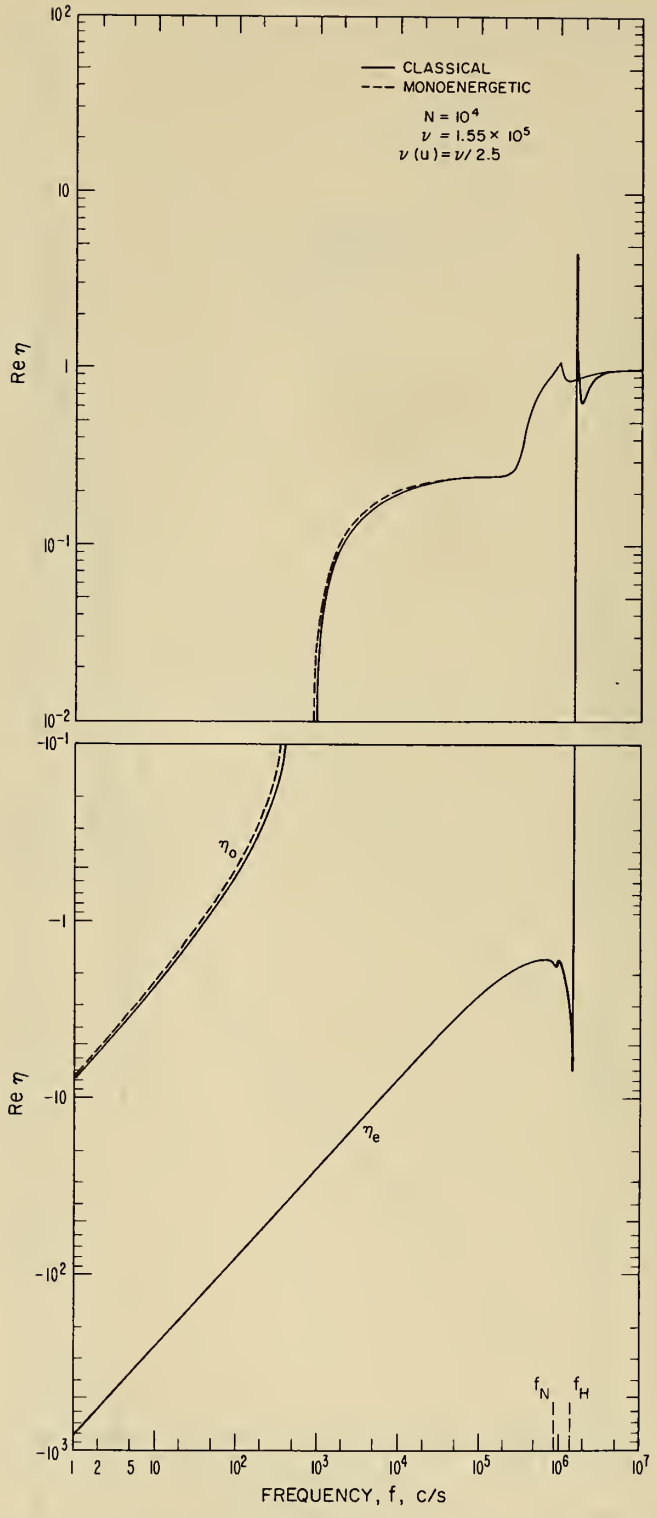

Fig. 24. Real part of complex index of refraction, Re η, of the lower ionosphere for upgoing ordinary (o) and extraordinary (e), propagation components, illustrating the comparison of values based on the classical magneto-ionic theory with those based on the monoenergetic theory.

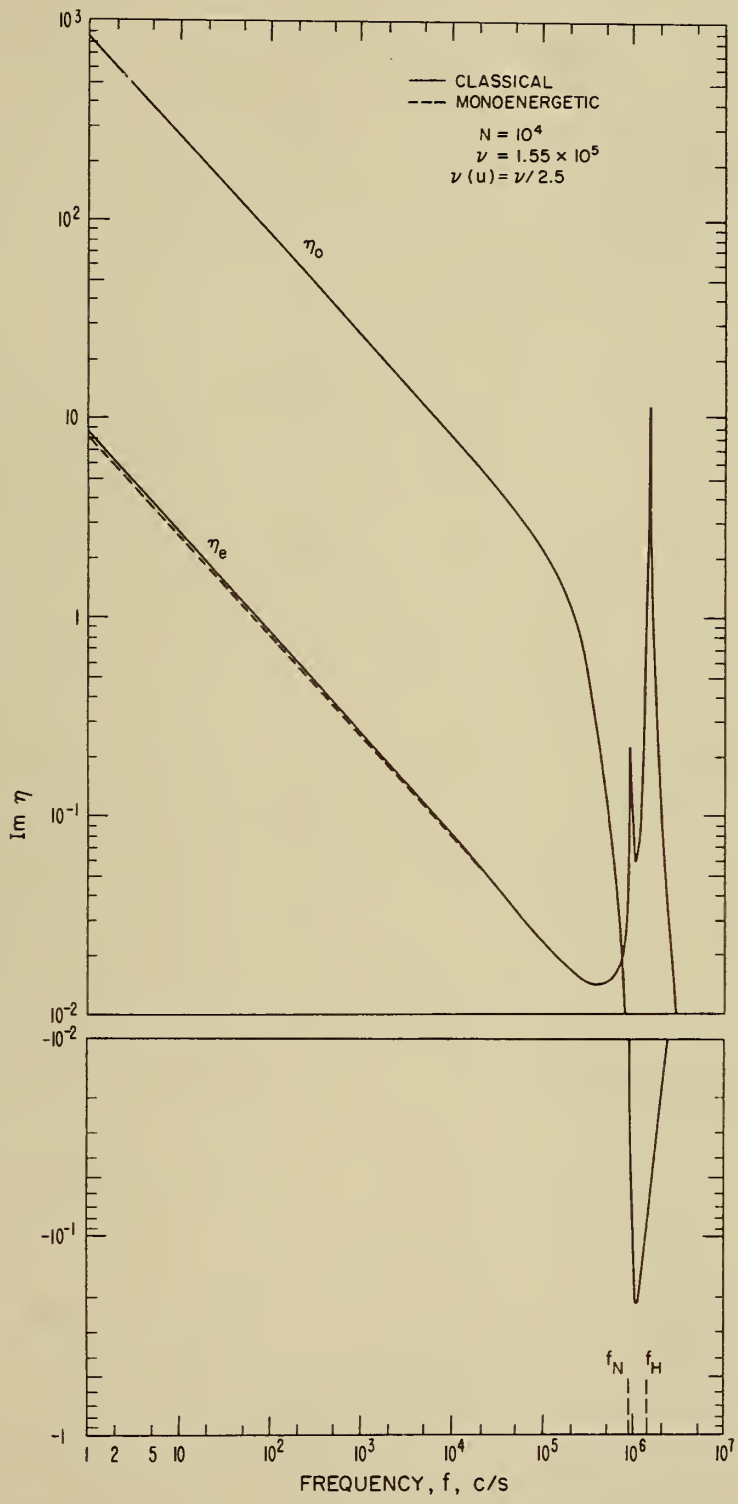

Fig. 25. Imaginary part of complex index of refraction, Im η, of the lower ionosphere for upgoing ordinary (o) and extraordinary (e), propagation components, illustrating the comparison of values based on the classical magneto-ionic theory with those based on the monoenergetic theory.

☆ U.S. GOVERNMENT PRINTING OFFICE : 1963 O - 679589

U. S. DEPARTMENT OF COMMERCE
Luther H. Hodges, *Secretary*

NATIONAL BUREAU OF STANDARDS
A. V. Astin, *Director*

THE NATIONAL BUREAU OF STANDARDS

The scope of activities of the National Bureau of Standards at its major laboratories in Washington, D.C., and Boulder, Colorado, is suggested in the following listing of the divisions and sections engaged in technical work. In general, each section carries out specialized research, development, and engineering in the field indicated by its title. A brief description of the activities, and of the resultant publications, appears on the inside of the front cover.

WASHINGTON, D. C.

Electricity. Resistance and Reactance. Electrochemistry. Electrical Instruments. Magnetic Measurements. Dielectrics. High Voltage.

Metrology. Photometry and Colorimetry. Refractometry. Photographic Research. Length. Engineering Metrology. Mass and Scale. Volumetry and Densimetry.

Heat. Temperature Physics. Heat Measurements. Cryogenic Physics. Equation of State. Statistical Physics.

Radiation Physics. X-ray. Radioactivity. Radiation Theory. High Energy Radiation. Radiological Equipment. Nucleonic Instrumentation. Neutron Physics.

Analytical and Inorganic Chemistry. Pure Substances. Spectrochemistry. Solution Chemistry. Standard Reference Materials. Applied Analytical Research. Crystal Chemistry.

Mechanics. Sound. Pressure and Vacuum. Fluid Mechanics. Engineering Mechanics. Rheology. Combustion Controls.

Polymers. Macromolecules: Synthesis and Structure. Polymer Chemistry. Polymer Physics. Polymer Characterization. Polymer Evaluation and Testing. Applied Polymer Standards and Research. Dental Research.

Metallurgy. Engineering Metallurgy. Microscopy and Diffraction. Metal Reactions. Metal Physics. Electrolysis and Metal Deposition.

Inorganic Solids. Engineering Ceramics. Glass. Solid State Chemistry. Crystal Growth. Physical Properties. Crystallography.

Building Research. Structural Engineering. Fire Research. Mechanical Systems. Organic Building Materials. Codes and Safety Standards. Heat Transfer. Inorganic Building Materials. Metallic Building Materials.

Applied Mathematics. Numerical Analysis. Computation. Statistical Engineering. Mathematical Physics. Operations Research.

Data Processing Systems. Components and Techniques. Computer Technology. Measurements Automation. Engineering Applications. Systems Analysis.

Atomic Physics. Spectroscopy. Infrared Spectroscopy. Far Ultraviolet Physics. Solid State Physics. Electron Physics. Atomic Physics. Plasma Spectroscopy.

Instrumentation. Engineering Electronics. Electron Devices. Electronic Instrumentation. Mechanical Instruments. Basic Instrumentation.

Physical Chemistry. Thermochemistry. Surface Chemistry. Organic Chemistry. Molecular Spectroscopy. Elementary Processes. Mass Spectrometry. Photochemistry and Radiation Chemistry.

Office of Weights and Measures.

BOULDER, COLO.

Cryogenic Engineering Laboratory. Cryogenic Equipment. Cryogenic Processes. Properties of Materials. Cryogenic Technical Services.

CENTRAL RADIO PROPAGATION LABORATORY

Ionosphere Research and Propagation. Low Frequency and Very Low Frequency Research. Ionosphere Research. Prediction Services. Sun-Earth Relationships. Field Engineering. Radio Warning Services. Vertical Soundings Research.

Radio Propagation Engineering. Data Reduction Instrumentation. Radio Noise. Tropospheric Measurements. Tropospheric Analysis. Propagation-Terrain Effects. Radio-Meteorology. Lower Atmosphere Physics.

Radio Systems. Applied Electromagnetic Theory. High Frequency and Very High Frequency Research. Frequency Utilization. Modulation Research. Antenna Research. Radiodetermination.

Upper Atmosphere and Space Physics. Upper Atmosphere and Plasma Physics. High Latitude Ionosphere Physics. Ionosphere and Exosphere Scatter. Airglow and Aurora. Ionospheric Radio Astronomy.

RADIO STANDARDS LABORATORY

Radio Physics. Radio Broadcast Service. Radio and Microwave Materials. Atomic Frequency and Time-Interval Standards. Radio Plasma. Millimeter-Wave Research.

Circuit Standards. High Frequency Electrical Standards. High Frequency Calibration Services. High Frequency Impedance Standards. Microwave Calibration Services. Microwave Circuit Standards. Low Frequency Calibration Services.


NBS